STUDY OF COPPER(I) THIOCYANATE LAYER AS HOLE TRANSPORT MATERIAL FOR SOLAR CELL APPLICATION

NURHAZWANI BINTI IZLAN

UNIVERSITI TEKNIKAL MALAYSIA MELAKA

STUDY OF COPPER (I) THIOCYANATE LAYER AS HOLE TRANSPORT MATERIAL FOR SOLAR CELL APPLICATION

NURHAZWANI BINTI IZLAN

This report is submitted in partial fulfilment of the requirements for the degree of Bachelor of Electronic Engineering with Honours

Faculty of Electronic and Computer Engineering
Universiti Teknikal Malaysia Melaka

2021

DECLARATION

I declare that this report entitled “Study of Copper(I) Thiocyanate Layer as Hole transport material for Solar Cell Application” is the result of my own work except for quotes as cited in the references.

Signature : …… …….

Author : Nurhazwani Binti Izlan

Date : 2 August 2021

APPROVAL

I hereby declare that I have read this thesis and in my opinion this thesis is sufficient in terms of scope and quality for the award of Bachelor of Electronic Engineering with Honours.

Signature	:	……	……
Supervisor Name	:	Puan Siti Aisah Binti Mat Junos @ Yunus	
Date	:	3 Ogos 2021	

DEDICATION

Thanks to Allah for paving the way for all that I have achieved. This thesis was entirely dedicated to my beloved parents and my supportive supervisor, who are my source of inspiration and provide great moral, emotional, and caring support. Finally, my family, friends, and colleagues, who help me to finish and always give me the opportunity to complete this project.

ABSTRACT

In this study, the performance of Copper(I) Thiocyanate (CuSCN) layer as hole transport material for solar cell applications was explored using SCAPS-1D simulation software. In this project, the completed simulated device construction is made of FTO / TiO_2 / N719/ CuSCN/ Ni. In orders to achieve the highest efficiency for solid-state dye-sensitized solar cell (SSDSSC) and the effect of back contact, several key parameters of hole transport layer (HTL) such as thickness, doping, working temperature, and defect interface layer were evaluated. Electron transport layer (ETL) like TiO_2, ZnO and SnO_2 have also been studied. The quantum efficiency was also investigated for a few parameters, instead of assessing the efficiency of the SSDSSC. The results proved that SSDSSC with back contact delivers a better performance compared to without back contact because of the low thickness of HTL. Furthermore, it can be shown that TiO_2 as ETL achieved the best output efficiency of 2.56%. The simulation findings can be utilized as a guidance in the SSDSSC fabrication process with CuSCN as a hole transport layer.

ABSTRAK

Dalam kajian ini, prestasi lapisan Tembaga (I) Thiocyanate (CuSCN) sebagai bahan pengangkutan lubang untuk aplikasi sel suria dieksplorasi menggunakan perisian simulasi SCAPS-1D. Dalam projek ini, pembinaan peranti simulasi yang lengkap dibuat dari FTO/ TiO_2/ N719/ CuSCN/ Ni. Untuk mencapai kecekapan tertinggi untuk sel solar peka keadaan pepejal (SSDSSC) dan kesan sentuhan belakang, beberapa parameter utama lapisan pengangkutan lubang (HTL) dinilai. Lapisan pengangkutan elektron (ETL) seperti TiO_2, ZnO dan SnO_2 juga telah dikaji. Kecekapan kuantum juga diselidiki untuk beberapa parameter, bukannya menilai kecekapan SSDSSC. Hasilnya membuktikan bahawa SSDSSC dengan kontak belakang memberikan prestasi yang lebih baik berbanding tanpa kontak belakang kerana ketebalan HTL yang rendah. Selanjutnya, dapat ditunjukkan bahawa TiO_2 sebagai ETL mencapai kecekapan output terbaik sebanyak 2.56%. Penemuan simulasi dapat digunakan sebagai panduan dalam proses fabrikasi SSDSSC dengan CuSCN sebagai lapisan pengangkutan lubang.

ACKNOWLEDGEMENTS

Above all, I thank Allah S.W.T for the blessings and encouragement that allow this work to be carried out.

I would like to express my deepest gratitude to my supportive supervisor, Puan Siti Aisah Binti Mat Junos @Yunus and Ts Dr. Faiz bin Arith, for their countless effort and help me to complete projects and their precious time that they gave me for finishing my project successfully. I am very thankful for their encouragement and peace during the whole process, especially in this new norm (Covid-19). It has been a great pleasure and honor to have them as my supervisor.

Besides, I would also like to thank my supportive parents and my helpful friends, for their ongoing support and affection, which keeps me inspired and focused all the time.

TABLE OF CONTENTS

LIST OF FIGURES

LIST OF TABLES

LIST OF SYMBOLS AND ABBREVIATIONS

CuSCN	:	Copper (I) Thiocyanate
SSDSSC	:	Solid-state Dye sensitized Solar Cell
SCAPS	:	Solar Cell Capacitance Simulator
ETL	:	Electron Transport Layer
HTL	:	Hole Transport Layer
TiO_2	:	Titanium Dioxide
FTO	:	Fluorine-doped Tin Oxide
CdTe	:	Cadmium Telluride
HTM	:	Hole Transporting Material
Ni	:	Nickel

CHAPTER 1:

INTRODUCTION

This chapter explains about the subject matter and problems statement, objectives, the scope of work, and significance of the project. The project background and problem statement will be introduced in this chapter regarding the challenges for simulating the hole transport layer for solid-state dye-sensitized solar cells application. The outline of the thesis summary is included by the end of the chapter.

1.1 Background Study

Nowadays, fossil fuels which cover 85% of our overall energy consumption, are the primary source of energy. It is known as non-renewable electricity that will one day be replenished. Excessive use of fossil fuels has a detrimental effect on the atmosphere due to the accelerated loss of ozone, the emission of greenhouse gases and other dangerous environmental pollutants[1] . Although the planet is suffering from global warming, clean energy options, such as water, wind, solar, biomass and hydro, will be the perfect way to reduce the effects of carbon of various possibilities. One of the benefits of clean energy is that it does not release greenhouse gases or radioactive waste into power generation. In the last two decades, the addition of solar energy to global energy production has risen dramatically. With a growing population and an increased standard of living, energy is required to power commodities.

Solar energy is a category of green energy that is sustainable, limitless, and therefore non-polluting. Solar energy is the main sources of energy used to substitute fossil fuels due to affluence. The utilization of energy of the Sun continues by reflecting the rays of the Sun with glass and the mirrors on the light, and so now the cars, houses and water supplies are solar powered. The energy of the Sun is free, but the system used to transform this energy is not free. There has been a great deal of study and invention on various methods to exploit the power of the Sun. However, the available technology accounts for just one-tenth of one per cent of global energy demand.

Solar cell is referred to as a photovoltaic cell, a device that can transform light energy as a source of electrical energy by photovoltaic effects. The process used to produce electricity using semiconductors is called photovoltaics (PV), which displays the photovoltaic effect by transforming solar radiation to direct current electricity. The photovoltaic effect is the mechanism of creating electrical voltage when light or other radiant energy enters two separate contact materials[1]. Power is generated by the electrical voltage and current of the solar cell. The commercialized solar cells are high efficiency, but the price is very high especially silicon (Si). It is the most common type of semiconductor used for production of solar cells and other electronic equipment. The solar cell is also a semiconductor device capable of creating 14 electrons free of charge. The same solar energy wavelength is absorbed while the creation of a free electron happens. There are currently three forms of solar cell generation on the market that used to tap the energy of the Sun. First-generation solar cells have a more substantial market share relative to other years. It is thanks to high conversion performance and good industry.

The applications of solar cell are used in calculators, certain smartphone, and watches. Sufficient household energy can be produced by adding number of solar cells into array. Thus, the performance solar cells can be calculated by their efficiency in transforming light energy to electrical energy. Efficiency relies on properties of the substance that shaped the cell. Following the conversion of sunlight into energy, the average commercial solar cell has a capacity of 15%, and the upper limit of silicon solar cell performance is 29%, which is comparatively high than the highest laboratory, which is 25% [2].

1.2 Problem Statement

Considering the rising worldwide demand for energy and adverse environmental effects as far as conventional energy sources are concerned, it is apparent that the production of clean and renewable energy is a matter of necessity. Besides, the third generation of the solar cell such as solid-state dye-sensitized solar cell has been introduced since it utilizes a low-cost production and offers higher stability and reliability. However, the power conversion efficiency is relatively low. Thus, it has been noticed that the p-type inorganic semiconductor as a charge selective material or a charge transport material shows a significant impact on solar cell performance.

Copper(I) Thiocyanate are commonly used for p-type semiconductor materials in new generation of solar cells. It is ideal for low temperature, inexpensive and flexible processing methods. Therefore, the p-type study materials are important to rationally design an efficient SSDSSCs CuSCN as inorganic p-type material as a replacement to find the best parameter for SSDSSC and the effect of the parameter by simulating CuSCN as hole transport material by using SCAPS 1D simulation software.

1.3 Objectives

There are some objectives that need to be accomplished for this project. The objectives are set out below:

i. To simulate the CuSCN as inorganic p-type material for a solar cell using SCAPS software.
ii. To analyze the output of simulated solar cell.
iii. To study the influence of CuSCN to the cell performance.

1.4 Scope of Work

At the beginning of this project, the focus is to understand the fundamental of solar cell structure and the SCAPS simulation software by doing background research on the cell structure and software. Next, design the solar cell using CuSCN as hole transport layer based on the SCAPS input parameter numerical analysis for SSDSSC. In this research, the entire simulated device structure consists of five layers: FTO/TiO_2/N719/CuSCN/Ni. Several crucial HTL characteristics, as well as the impact of back contact, have been investigated in orders to attain the best efficiency for SSDSSC. The parameters discussed previously include the incorporation of ETL layer such as TiO_2, ZnO and SnO_2, CuSCN thickness, CuSCN doping acceptor density, solar cell working temperature, and various material of back contact and defect interface layer at CuSCN/N719 and N719/TiO_2. Instead of analyzing the performance of SSDSSC, the quantum efficiency of different absorbent layer was further analyzed to obtain an optimum performance of SSDSSC. In this study, only the J-V curve will be used to determine the Power Conversion Efficiency (PCE).

1.5 Thesis Outline

In this thesis, there will contain five chapters to describe the project entitled Study of Copper (I) Thiocyanate (CuSCN) layer as Hole Transport Material for Solar Cell Applications. At first chapter is Introduction and followed by Background Study, Methodology, Result and Discussion, and the last chapter is Conclusion. The summary of the content for each chapter shown below:

Chapter 1 – Introduction of the project explained an overview about the solid-state dye-sensitized solar cell and solar cell. This chapter covers the Introduction of the

project title, problem statement, objectives to be achieved by the end of the project and the scope of work when implementing this project.

Chapter 2 – In this chapter consist of the history analysis and research study lead to the formation of this project. In addition, the background study contains the fundamental of the solid-state dye-sensitized solar cell and the previous work related to this project.

Chapter 3 – Methodology chapter will describe the methods and equipment that use in this project. The flowchart is necessary for this chapter to arrange the steps in this project development.

Chapter 4 – Results and Discussion. For chapter 4, it will present the findings and analysis from the project. There are two properties that observe and measure to obtain better efficiency, which is structural and electrical. Different properties use different equipment to obtain the analysis and results. The efficiency of SSDSSC can be determined by using the given equation.

Chapter 5 – Conclusion and Future Work. This chapter will discuss the Conclusion that can be drawn from the project. Therefore, it also consists of a summary of the project and will discuss the recommendations for future work purposes which can be improved in some ways to obtain better results and performance.

CHAPTER 2:

BACKGROUND STUDY

This chapter covers the literature review of the project. In this chapter, it discusses the previous works that include the information gathered to obtain knowledge and ideas for the project's completion. Several sources, such as books, thesis, and journal, have taken as a resource for this project. Method and approaches that used also take from the resource as reference and guideline.

2.1 Introduction

2.1.1 Basic of Solar Cell

A solar cell is a main component that transforms light energy to electrical energy for the conversion of photovoltaic energy. Such as, the semiconductor used for the application of solar cell material. The energy transfer contains of the absorption of the electron-hole pairs of light (photon) energy in the semiconductor and the separation of the load carrier [3]. Solar is a healthier, better investment for our family and company. It also immediately reduces the power bill, experience, energy freedom from increasing energy prices and raise carbon dioxide (CO_2) emission and increase the value of our home or house [4]. The solar cell will continue to generate power forever as the Sun is shining. The solar cell is truly a sustainable and environmentally friendly means of generating electricity. In most cases p–n junction is used for separation carrier charges. It is necessary to learn the basic properties of the semiconductor and the theory of traditional p–n solar cell junction in orders to understand not only the conventional solar cell, but also the modern type of solar cell [3]. Besides, the comprehension of the p–n solar cell junction will bring you hints to boost solar cells in terms of performance, cost of output, energy usage.

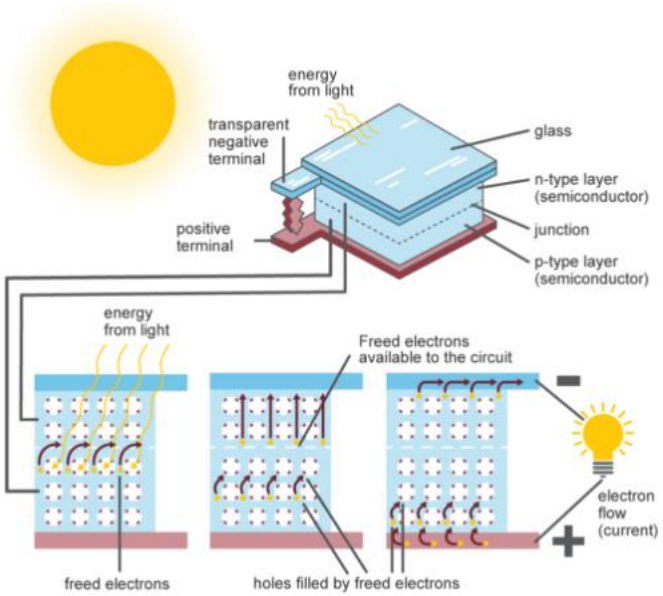

Figure 2.1: Shows the inside of the photovoltaic cell [3].

Thus, three generations of solar cells and the first generation is relatively expensive and low efficiency solar cells. The second generation of solar cells is cheaper to produce but less effective since the price per watt is lower than the cells of the first generation. Besides, the third generation of solar cells are very efficient as there are researcher taking places in this generation even most of the technologies in this generation are not commercialize yet. The aim of the third generation is producing cheaper solar cells with high efficiency[5].

2.1.1.1 First Generation Solar Cells

Basically, for the first generations of solar cell contains crystalline silicon (c-Si) or Germanium doped in PN-junction with phosphorus and boron. Crystalline silicon solar cell can achieve high power conversion efficiency however the fabrication process is high cost due of using sophisticated equipment. The most effective photovoltaic devices in a single cell are silicon solar cells. It is ideal for 1.1 eV energy band gap photovoltaic applications [5]. The solar cells in this

generation are made of thin silicon wafers and called monocrystalline solar cells because the cells are formed from large single crystals [6].

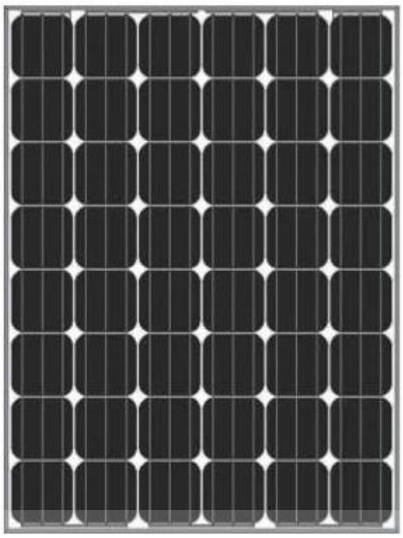

Figure 2.2: Monocrystalline solar cells.[6]

2.1.1.2 Second Generation Solar Cells

Second generation solar cells defined as thin film solar cells, because there are only a few micrometers thick when compared to crystalline silicon-based cells. [7]. Theoretically, the thin-film solar cells may provide less cost effectives electricity than solar cells based on c-Si. Thin-film solar cells are made up of a series of thin films placed over a broad, low-cost substrate like glass, polymer, or metal. Thin films can be bundled into flexible, light structures that can readily be integrated into building components.

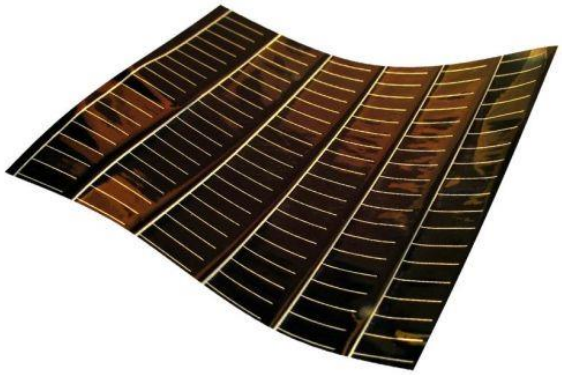

Figure 2.3: Cadmium Telluride [7].

2.1.1.3 Third Generation Solar Cells

Due to the high costs and toxicity of first-generation solar cells, as well as limited material availability for second-generation solar cells, a new generation of photovoltaic cells has arisen. Because they are not dependent on the construction of the other p-n junctions, third generation solar cells are essentially different from the prior two generations. This new generation of solar cells is constructed of a variety of different materials, including nanomaterials, silicon wires, solar inks printed on normal printing presses, organic dyes, and conductive polymers, in addition to silicon [8]. DSSC is more efficient across a wider range of solar energy, is less expensive, and is non-toxic, allowing it to be used by a larger number of people and expand its applications [9]. DSSC is also high in efficiency, inexpensive in cost, simple to manufacture, environmentally friendly, transparent, and has good plasticity.

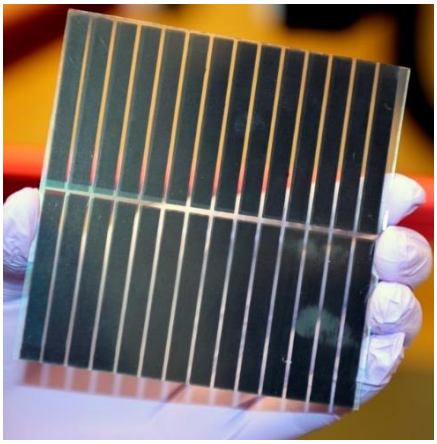

Figure 2.4: Perovskite Solar Cell [9].

2.1.1.4 The efficiencies first, second and third generations of solar cells

Different generation of solar cells produced different efficiency. All the efficiencies must be compared among each other to improve the production of solar cells from time to time.

Table 2.1 : Solar cell efficiencies[6][7][9]

Materials	Efficiency (%)	Area (cm^2)	Voc (V)	Jsc (mA/m^2)	Fill factor. (%)
Si (crystalline cell)	25.6	143.7	0.740	41.8	82.7
Si (multi-crystalline cell)	21.3	242.74	0.6678	39.80	80.0
Si (amorphous cell)	10.2	1.001	0.896	16.36	69.8
CIGS (cell)	21	0.9927	0.757	35.70	77.6
CdTe (cell)	21.0	1.0623	0.8759	30.25	79.4
Perovskite (cell)	19.7	0.9917	1.104	24.67	72.3
Dye (cell)	11.9	1.005	0.744	22.47	71.2

2.1.2 Copper(I) thiocyanate (CuSCN)

CuSCN is solid-ionized copper molecular which characteristics have been researched since the very first half of the 20th century [10]. Pseudohalide is a polyatomic group that includes pseudo halogen anion, for example thiocyanate, and is defined such a familiar with halide ions into organic compounds. CuSCN is a cheap and readily stocks commodity provided by major foreign manufacturers to laboratories. The structural features of CuSCN depending on the preparation method; CuSCN can be precipitated from a solvent in two ways; it is the α-phase and the β-phase which determine the properties of the substance especially angles of bond. For α phase will have a crystal orthorhombic lattice, while the β-phase may have been hexagonal or rhombohedral design. [10]. However, several research indicates the polymorphic structures between two phase can be detected, a thin films usually show β-phases [11]. Apart from that, CuSCN is a natural semiconductor materials that show conductivity of p-type as solid formulated in a solution in which the concentration of thiocyanate ions is greater than those of copper ions [12]. Therefore, this approach resulted in a molar ratio deficiency of copper atoms in the solid, and a hole-transporting character in p-CuSCN is caused by a copper vacancy in the crystal lattice, with an acceptor impurity level formed near valence band. Thus, the copper defect arrangement adds to its optical clarity, as the elimination of copper atoms from the ideal crystal lattice widens the optical bandgap [13]. Conversely, the stoichiometric abundance of copper atoms has the opposite effect and promotes increased N-type conductivity. In addition, CuSCN exhibits outstanding thermal stability because the decomposition of the substance into copper sulfide is observed only at temperatures above 300 °C [14].

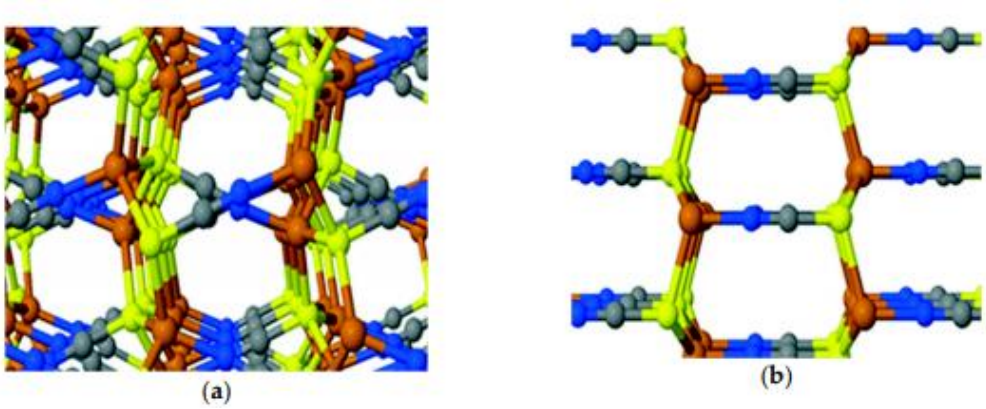

Figure 2.5: Shows the bulk three-dimensional phases of CuSCN: (a) α-phase (orthorhombic); (b) β-phase (hexagonal) where brown sphere = Cu; yellow sphere = S; gray sphere = C; and blue sphere = N [15][14].

2.1.3 Hole transport layer of CuSCN

Since the stoichiometric CuSCN was considered intrinsic in hole-carrying semiconductor, the extrinsic of p-type conductivity at room temperature was found which is related to development of impurity acceptor levels close to the peak valence band due to the prevalence of copper vacancy in the crystal lattice [6]. Thus, hole mobility field effects value is up to 0.1 $cm^2V^{-1}s^{-1}$ has recently been recorded for TFTs based on the CuSCN nanocrystalline film solution [13]. It has been proved that devices produced and tested in inert atmosphere display inherent holes transporting properties, but a major p-type doping effect has been observed for a few days after exposure of transistors to air [16]. Thus, to the external doping results CuSCN holes transport characteristics are often known to be strongly dependent with manufacturing conditions as well as on chip structure, electrode interface resistance and dielectric/semiconductor trap density design [17]. Thus, the fundamental physical processes are yet to be studied and understood, and further study is needed. Therefore, this implies while the maximum recorded hole mobility in CuSCN is below that of the most effective p-type semiconductors at present, optimization of manufacturing

parameters could potentially lead to a significant increase in the holes transport properties of CuSCN thin film.

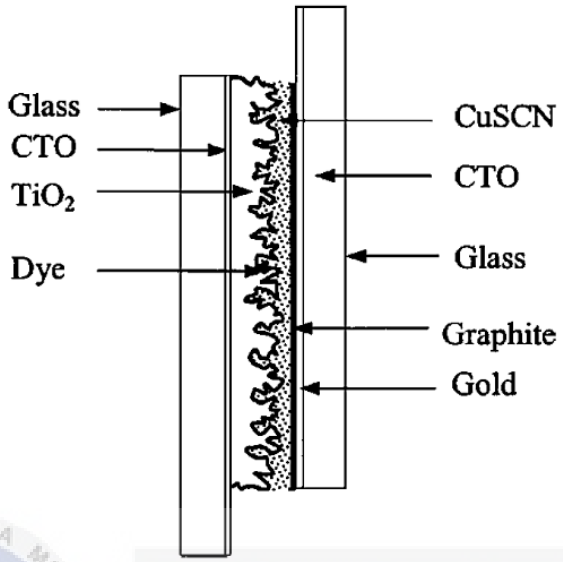

Figure 2.6: Shows the dye-sensitized NIR photodetector with n-TiO_2; p-CuSCN is used as the hole conductor [18].

2.1.4 Solid State Dye-Sensitized Solar Cell (SSDSSC)

A solid-state dye-sensitized solar cell (SSDSSC) is a simplified combination of dye-sensitized solar cells (DSSC) where liquid electrolyte is based systems have not been commonly used in the commercial industry due to concerns about solvent leakage and corrosion issues due to iodide/triiodide redox couples. Various techniques have been studied for the substitution of liquid electrolytes, that is polymer electrolytes, ionic liquids, p-type inorganic semiconductors such as CuI or CuSCN, and organic hole conductors.[19]. The SSDSSC is like other solar cells that effectively produces photovoltaic electricity.

Dye sensitizer is immobilized by linking its functional group to a wide-band, n-type semiconductor gap such as zinc oxide or titanium dioxide [20]. Dye sensitizer is initially in the ground state and can be excited to the lowest unoccupied molecular orbital state as light is absorbed. The excited dye then emitted electrons to the metal oxide matrix conduction band. Around the same time, the holes are accumulated in the oxidized dye, producing a moment of load separation, the electron is in the semiconductor while holes in the oxidized dye. However, semiconductor enables the accelerated diffusion of electrons to the FTO electrode [21]. Electrons are transmitted to the counter electrode, and HTM absorbs electrons while the holes are passed to the counter electrode by electrical conduction from the solid hole species. [22]. The oxidized dye will receive electrons from HTM to restore its ground state within several hundred picoseconds, returning to the original condition before the photon excitation.

The regeneration of SSDSSC dye is in orders of magnitude being faster than the liquid form cells that require microseconds to regenerate. It is because the fact that the liquid mechanism is restricted by the diffusion limit, rather than enabled by the direct transfer of the hole that induces the injection of the hole and the injection of the electron through the HTM-dye or metal oxide matrix occurs simultaneously[22][23]. After that, the system is then able to resume all the process over again.

2.1.5 Basic principle of Solid-State Dye-Sensitized Solar Cells

A thin, compact film of TiO_2 is deposited on conductive substrate glass, typically coated with fluorine-doped tin oxide (FTO), supplemented with the mesoporous layer of TiO_2. Although the conventionally used spiro-OMeTAD as HTM, the mesoporous layer is relatively thin around 3 μm [24]. The thick TiO_2 layer prevents direct contact between the FTO and the HTM, which could lead to a loss due

to shunting (holes in the HTM and electrons in the FTO could recombine). The color of molecules was absorbed to the surface of the TiO_2. Next, HTM is penetrated to the porous framework, whereas a thin HTM overlay is developed. The metal effect is eventually evaporated at the top of the HTM. Thus, when the metal direct contact with TiO_2, it can also lead to shunting. [19] A schematic drawing of the standard SSDSC computer layout is shown in the diagram below.

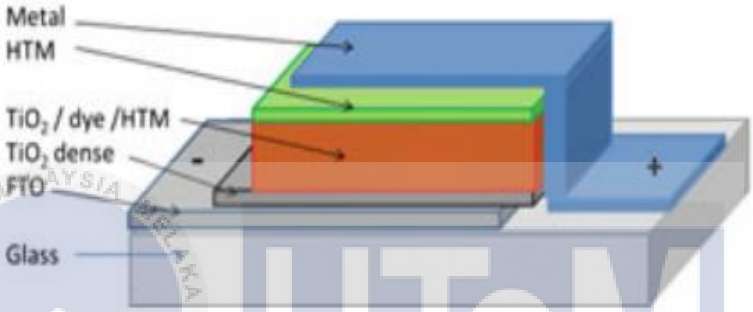

Figure 2.7: Shows the structure of a solid-state dye-sensitized solar cell [19].

The dye molecules absorbed photon, and therefore resulting excited molecules will attach the electron with conduction band of TiO_2. The oxidized dye receives an electron from the hole transfer material (dye regeneration). Following these initial load separation procedures, the electron transfer of the mesoporous TiO_2 film to the FTO substrate and the transport of the hole in the HTM sheet to the metal contact is conducted out. [25]. The dye of SSDSC also can be ultra-fast. Bach et al. registered a 50% hole injection at 900 ps for oxidized N3 in contact with spiro-OMeTAD [26].

The electron life is slightly shorter with 2 until 3 orders of magnitude compared to 1-DSC with the traditional iodide/triiodide redox mediator. As result, the electron

diffusion duration in SSDSC is significantly shorter than in l-DCC. Electrolytes of around one order of magnitude (~1 μs vs ~10 μs)[27]. In addition, electron transfer, calculated by tiny photocurrent modulation transients, has been observed and is significantly faster than 1-DCS with the same film thickness and photocurrent strength. [19].

2.2 Previous Work

2.2.1 CuSCN as Hole Transport Material (HTM)

The HTM is very crucial in SSDSSC to enhance charge transportation and extraction. A good HTM in high performance of solar cell should accept the holes from the light absorber efficiently, operate rapid transportation, and hole (HTM)-electron (TiO_2) recombination can be suppressed as much as possible. In this thesis, we are going to focus on CuSCN as HTM.

2.2.2 SCAPS-1D Simulation Software

The performance of SSDSSC with different HTL can be analyzed using a Solar Cell Capacitance Simulator (SCAPS) software in the one-dimensional configuration. A simulation in the behavior of multilayer's solar cell can be done using this software. There are many properties that can be analyzed and manipulated, such as thickness, temperature, bandgap, etc. The solar parameter efficiency can be determined from the simulation using SCAPS-1D software

2.2.2.1 Simulation using Copper(I) Thiocyanate

Hole transport material (HTM), a form of substance that prevents the electron transfer to the counter electrode in metals, produces barriers to prevent direct interaction between the metal electrode, the metal oxide matrix, and encourages the transfer of holes from the metal oxide matrix to the counter electrode. HTM is

basically a valve which favors electron as hole pairs in one direction, but it cannot be fully recombined [28]. Moreover, HTM higher holes mobility, low toxicity, and thermal stability to clean the SSDSSC during manufacturing. The highest occupied molecular orbital (HOMO) level energy should also match the electron generation component's valence band power and said that HTM should defend metal oxide and thinner layer against air and moisture and prevent the spread of external moieties or elements inside the photo-absorber area. Maybe the most significant aspect is that the HTM displays limited absorption in the visible and near-infrared range to eliminate the absorption of photons during the photo enthusiasm of excitons.

Referring to the journal by O'Regan *et. al* [29], explored that p-type CuSCN (Eg = 3.1 eV) as holes conductor in SSDSC. In previous work, CuSCN was deposited using electrodeposition [29], the solvent deposition of n-propyl sulfide was then used [30]. Thus, the efficiencies hit around 2% using the N3 dye [15]. After that, according to Premalal *et. al* [15], stated that the improvement CuSCN doping by application of trimethyl laminate and PCE by 3.4% using N719 dye. Thus, CuSCN has a band gap of 3.6 eV, the exposure of solid CuSCN to halogen gas as shown by Perera, Senevirathna *et. al* [24], will reduce it to 2.6 eV. This approach resolved the problem of conductivity of CuSCN as HTM, which is not high enough depending on the existence of excess SCN and prevents the inclusion of enough excess SCN in the CuSCN synthesis.

Next, based on research by Ranasinghe *et. al* [14], remarkably achieve a power conversion efficiency of 2.28% by building SSDSSC and FTO/ZnO thick layer configuration/ZnO porous layer configuration/D149/CuSCN/Graphite/Cr-coated FTO [14]. Optimized solar cells also have parameters estimated at an open circuit voltage

of 0.55 V, a fill factor of 0.51 and a short circuit current density of 8.2 mA/cm^2. However, the power conversion efficiency is relatively low. Therefore, further improvement is needed to improve the efficiency.

According to F. Jahantigh et. al [31], reported that CuI is 17.72% more effective in photovoltaic cells relative to CuSCN with a performance of 16.69% in inorganic HTMs. The ability to use secondary doping and to prepare compact solar cells is an important benefit of organic HTMs. Therefore, the findings reveal that SDSSCs are simulate with a thickness of 10 nm, 500 nm HTM and 3 nm of TiO_2. In this study, SCAPS software were used to model the actions of multi-layer solar cells. The properties of the cell vary by adjusting the features of each sheet for example, thickness, doping, bandgap, temperature, and dielectric constants [31].

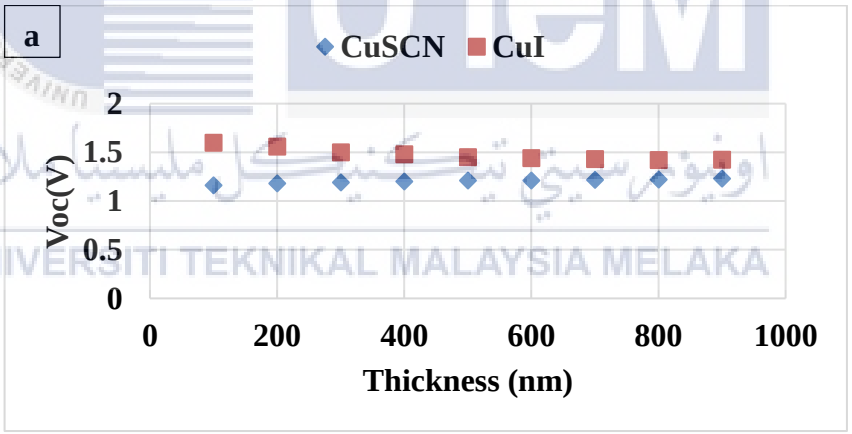

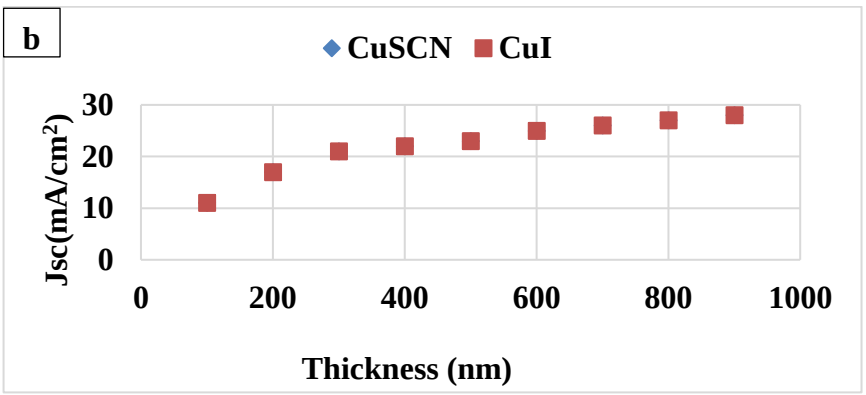

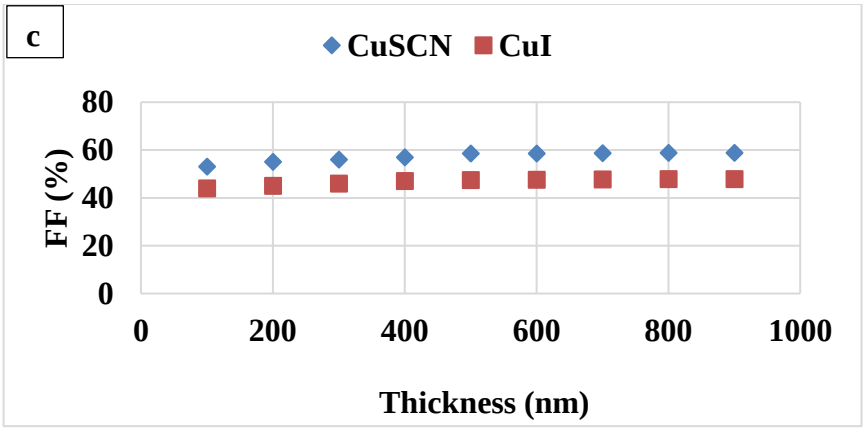

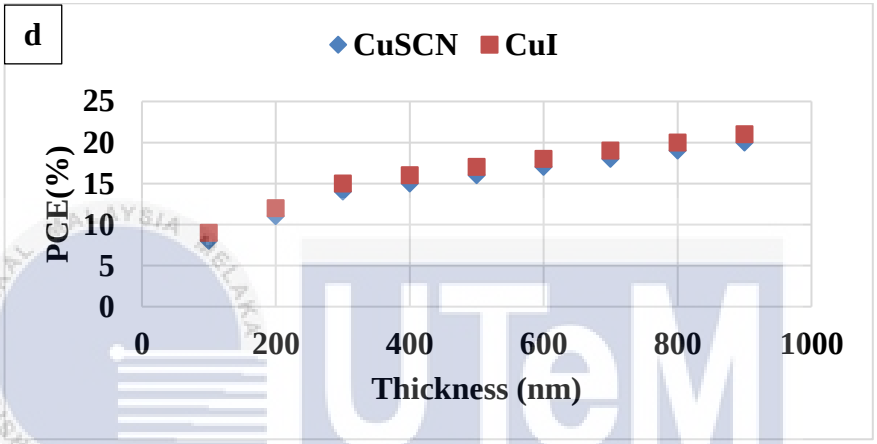

Figure 2.8: The effect of Holes Transport Material layer thickness on a) Voc, b) Jsc, c) FF% and d) PCE% of the SDSSC [31].

Table 2.2: The summarized performance of SDSSCs prepared with different HTMs [31].

HTM types	Voc (V)	Jsc (mA/cm^2)	FF (%)	Efficiency (%)
CuSCN	1.1975	24.582207	56.71	16.69
CuI	1.4981	24.725547	47.85	17.72

Based on the Table 2.2, the highest efficiency of CuI and an efficient of 17.72%, is highest photovoltaic cells compared to CuSCN with efficiency of 16.69% among

an inorganic HTMs. However, the ability to use secondary doping to prepare lightweight solar cells is also an important benefit of organic HTMs. Thus, the findings reveal that SDSSCs are simulated with 10 nm dye layer thickness, 500 nm HTM and 3 nm TiO_2 thickness. However, further studies need to be done for this research.

2.2.3 Parameters of efficiency

From previous researcher, there are four standard parameters are used to observe the performance of cell characteristics such as power conversion efficiency (η), fill factor (FF), current of short-circuit (Isc), and a voltage of open circuit (Voc).

2.2.3.1 Power conversion efficiency (PCE)

Solar cell performance is the main DSSC parameter as assigned to determine solar cell efficiency. The ratio of efficiency can be described and as power output by solar cells to the Sun's power supply. The continuum and hence intensity of the sunlight incident affected solar cell production. In essence, to compare the output of two and more solar cells, efficiency is calculated. Solar cell efficiency can be calculated as follows:

$$\text{Pmax} = \text{Voc} \times \text{Isc} \times \text{FF}, \text{Watt(W)} \quad \textbf{(2.1)}$$

$$\text{Efficiency}, \eta = \left[\frac{P_{max}}{P_{in} \times A}\right] \text{x } 100\% \quad \textbf{(2.2)}$$

2.2.3.2 Fill factor (FF)

The fill factor or parameter to measure the full capacity of solar cells is commonly referred to as "FF." FF is one of the main parameters for high performance of solar cells efficiency. Therefore, FF is calculated graphically on the maximum rectangular

region that suits curve in I-V. The FF is the ratio of V_{max} as well as I_{max} to the commodity V_{oc} and I_{SC} product. The V_{max} and I_{max} goods reflect the full strength of solar panel. The FF estimation equation as shown below:

$$FF = \frac{Im \times Vm}{Isc \times Voc} \quad \textbf{(2.3)}$$

2.2.3.3 Short circuit current (Isc)

For short circuit current, if the voltage is zero, the short circuit current is known as present in the solar cell. The short circuit current is normally written as I_{SC}. When produced, the short circuit current can be calculated if light exist. Below is the I-V curve for short circuit current.

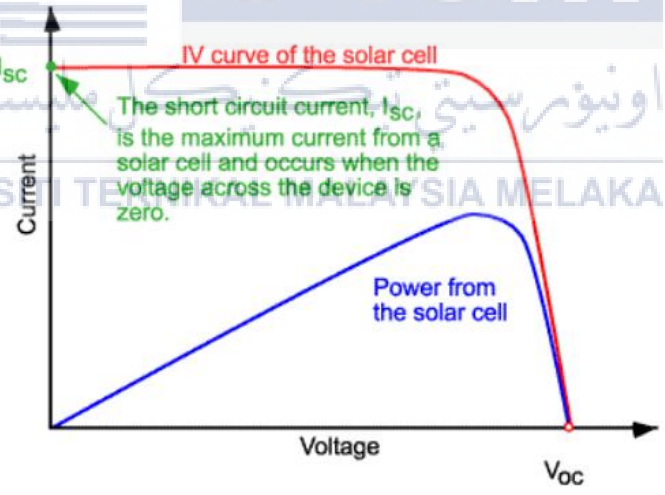

Figure 2.9 : Shows I-V curve of short circuit current [38].

2.2.3.4 Open circuit voltage (Voc)

The photovoltaic cell optimum voltage is the open circuit voltage (Voc). The voltage of the open circuit corresponds to the voltage forward solar cell bias regardless of the bias caused by the solar cell joint and daylight present current.

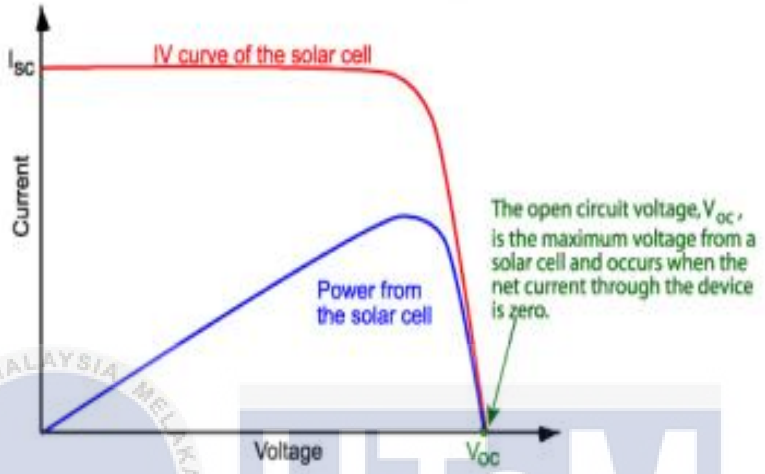

Figure 2.10: Shows I-V curve of open circuit voltage [38].

2.2.4 Fabrication of CuSCN films.

2.2.4.1 Spin coating method

According to Neeraj Chaudhary *et. al* [39], reported that CuSCN be used for solution-processed thin film deposition of organic solar cells utilizing environment safe and natural solvent dimethyl sulfoxide (DMSO). Two separate PCDTBT and PTB7 photovoltaic systems are produced utilizing a mixture of $PC_{71}BM$ as an approving material with ITO/CuSCN/Active Layer package structure [38]. Up to 4.20% and 3.64% of energy transmission quality PCE dependent on CuSCN, with a comparatively higher fill factor (FF) compared with previously published literature values were obtained with DMSO as the deposition solvent.

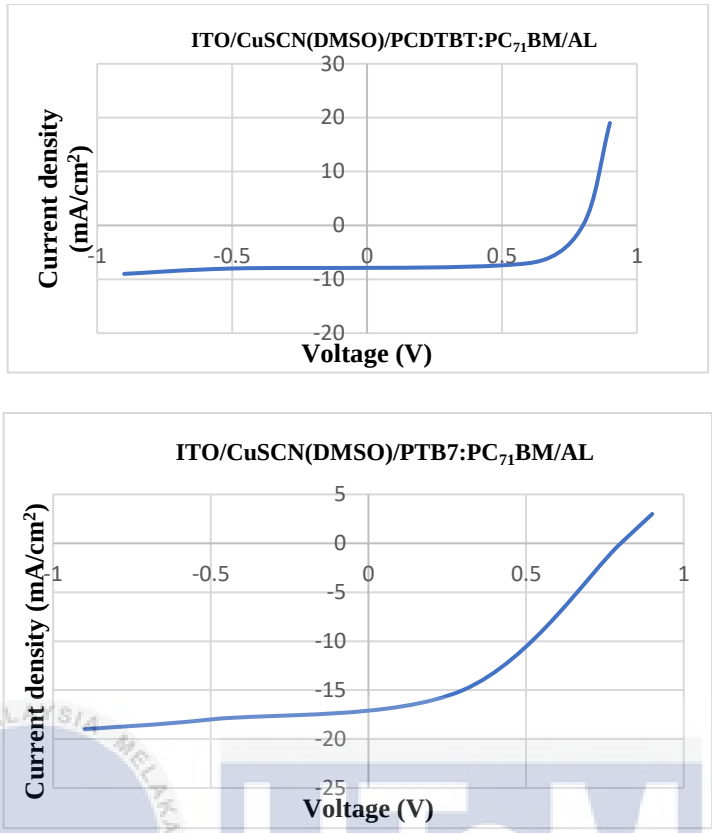

Figure 2.11 : Current density versus voltage (J-V) curves photovoltaic device[39].

Table 2.3 : Shows solar cells parameter[39]

Entry	Active materials	J_{sc} (mA/cm^2)	V_{oc} (V)	FF%	PCE%
1	PCDTBT: $PC_{71}BM$	10.55(±0.32)	0.72(±0.02)	54.98(±2.03)	4.20(±0.25)
2	PTB7: $PC_{71}BM$	16.7(±0.63)	0.60(±0.03)	36.41(±1.63)	3.64(±0.20)

Table above shows solar cells parameters of the devices from solution-processable CuSCN as HTL and donor materials with $PC_{71}BM$ of active area of 4 devices.

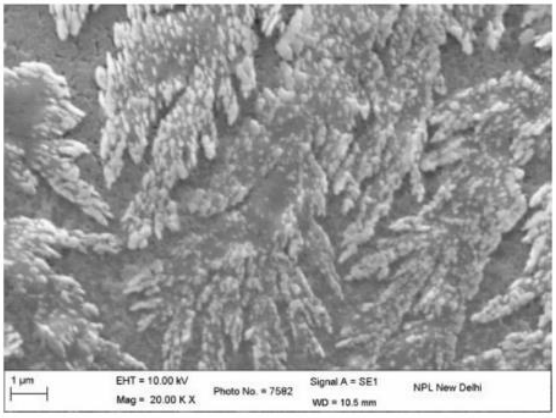

Figure 2.12 : Shows SEM image[39].

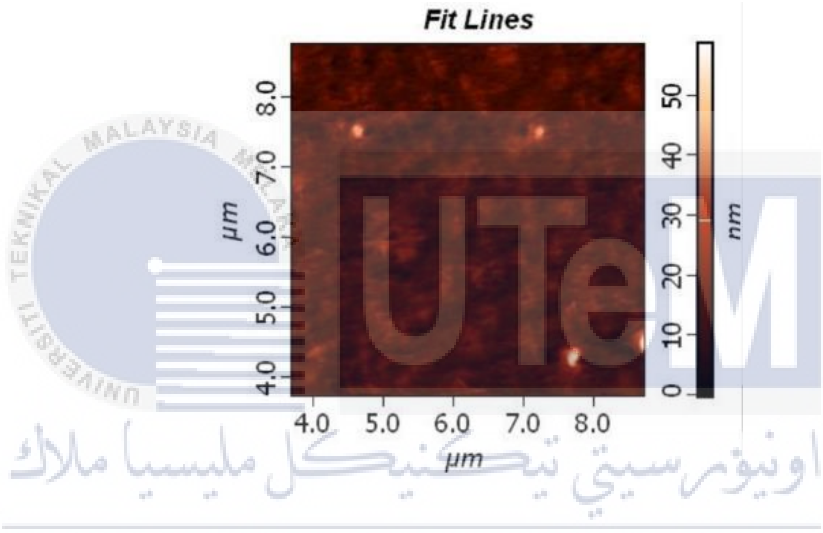

Figure 2.13: AFM images of CuSCN thin films deposited from DMSO solution on glass substrate [39].

Overall, the highest efficiency was achieved when solution-processable CuSCN as HTL materials with PCDTBT: $PC_{71}BM$ as an active material were used. Its efficiency was 4.20 ($\pm$0.25)% higher compared to PTB7:$PC_{71}BM$ as active material.

However, results revealed that spin-coating of CuSCN thin films was obtained from solvent DMSO and considered to be extremely clear. Photovoltaic equipment is produced with ITO/CuSCN/active layer system layout and up to 4.20% PCE. In addition, solvent DMSO offers compatible interface layers, which are equivalent to

dis-propyl sulfide and diethyl sulfide for producing organic solar cells that have disagreeable properties such as an unpleasant smell, adverse and irritant existence. Moreover, this is the first time CuSCN deposition using the DMSO solvent as HTL in efficient, organic solar cells is demonstrated as an environment-friendly solution-processable. The recommendations need more examples of an active layer with CuSCN as well as effective HTL inorganic solar cells cheap and solution-processable.

2.2.4.2 SILAR method

According to Blessing N. Ezealigo *et. al* [40], a cost effective SILAR process for depositing CuSCN nanoparticles on steel and glass were used in this analysis. In this study, all the chemicals used were analytical grade and include copper sulphate pentahydrate, sodium thiosulphate, sodium thiocyanate, sodium sulphate, and sodium thiocyanate [40]. For substrates, microscopic glass slide was cleaned with detergent then rinsed with distilled water, put 30 min in acetone, cleaned with distilled water again and then ultrasonicated for 20 min and rinsed again, after that the substrates were dried 20 min in sterilizing oven for 60 ℃. Next, kept in air-tight box to prevent contamination [40].

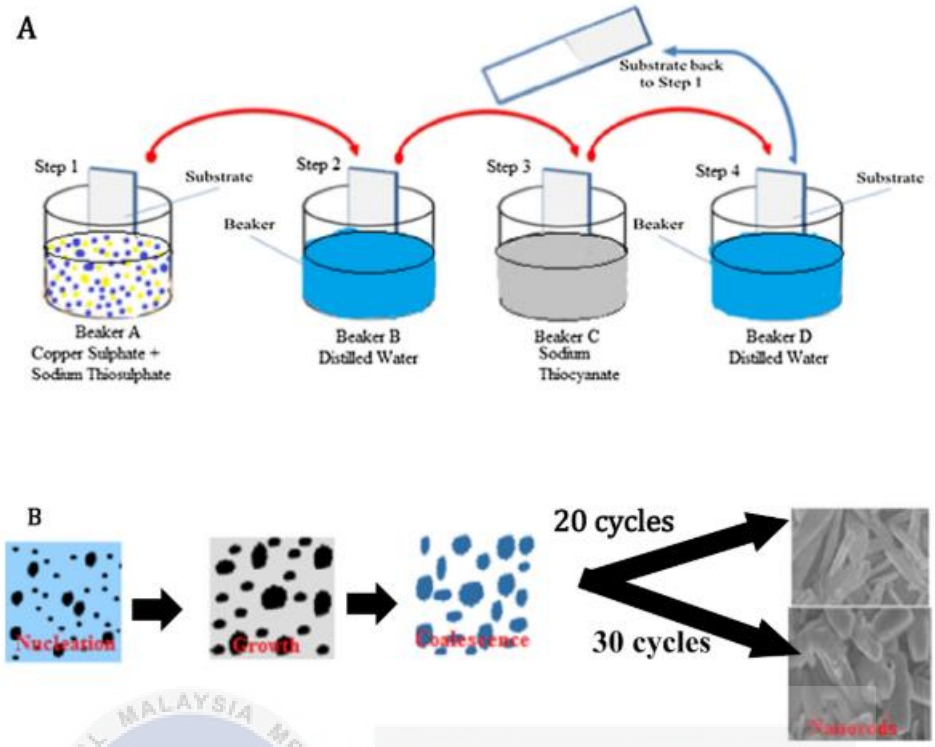

Figure 2.14: (A) Shows schematic diagram of SILAR deposition of CuSCN thin film, (B)Schematic formation of the nanorods of CuSCN deposition on steel and glass substrates[40].

Based on the figure above, 0.1 M of $CuSO_4$, the cationic precursor was dissolved in distilled water and complexed with 0.1 M of $Na_2S_2O_3$. From the figure above can see that the process of immersing the substrates through all four beakers gives a complete SILAR cycle. Next, the samples were dried in the oven for 10 min at 60 ℃ before been characterized. In this study, 20 and 30 deposition cycles were employed as to study the effect of number of cycles on the properties of the thin films.

Moreover, by referring to Prashant Kishor Baviskar [40], stated that the solar solid-state dye-sensitized photovoltaic performance parameters such as short-circuit

photocurrent density (Jsc) and open-circuit voltage (Voc), fill-factor (FF) and efficiency of power transmission under light of the 1 sun (100 mW/cm^2) have been measured for different CuSCN SILAR cycles and findings are summarized in Table 2.4. An improvement in the amount of SILAR CuSCN periods, the Jsc values are observed, and unit performance tends to improve to 30 cycles. Jsc's low values for a 10 and 20-cycle system may be attributed to a lack of CuSCN coverage over ZnO nanorod and to a weak pore filling effect, which is responsible for lower device efficiency [41]. For devices prepared at 30 cycles, optimum performance can be observed because of the full coverages of dye-sensitized ZnO nanorods with a flake-like CuSCN morphology that fills the pores and grows above 1 μm over ZnO nanorods provides the direct route for the transfer of charges. For 40 cycles, the decrease in output was observed which can be induced by the creation of a thick CuSCN layer that serves as a barrier to the transfer of charge. In addition, the latter debate is well supported by the values of sequence resistance (R_s) and shunt resistance (R_{sh})[42]. The values for series resistance and shunt resistance determined by the lighting relationships on the slope of the J-V curve.

Table 2.4: The photovoltaic output parameters of solid-state dye- sensitized solar cells with different SILAR cycles of CuSCN

No. of SILAR cycles for CuSCN	J_{sc} (mA/cm^2)	V_{oc} (mV)	R_s (Ω)	R_{sh} (kΩ)	FF (%)	Efficiency (%)
10	0.037	41.3	329	0.80	65.22	0.001
20	0.145	97.2	314	1.35	41.65	0.006
30	0.309	549	283	4.77	42.26	0.072
40	0.208	400	431	3.03	39.11	0.033

However, the development of solid-state dye sensitized solar cell (SS-DSSC) based on ZnO nanorods sensitized with low-cost Eosin-Y dye and CuSCN as a hole transport material is demonstrated effectively with simple SILAR technology at room temperature. For low-cost SSDSSC with structure FTO/ZnO seeds/ZnO nano rods/Eosin-Y/CuSCN/Au, maximal efficiencies are obtained at 0.072% at the sun (100 mW/cm^2) for 30 SILAR CuSCN cycles. Besides, the process used in this work will be used for wide scale applications, which would open the windows to prospects for the design and produce of SS-DSSC for various colors with a larger absorption covering in a noticeable range. Even though, as we can see from the Table 2.4, the performance efficiency is poor, but the FTO/ZnO seed/ZnO nanorods/EosinY/CuSCN/Au structure are still acts as SS-DSSC.

2.3 Table of comparison

Table 2.5: Shows summary of the fabrication of CuSCN as hole transport material.

Solvent used	Duration	Annealing Temperature	Deposition Method	Thickness(nm)	Efficiency %	Ref.
Dipropyl sulfide	4 hours	Room Temperature	Spin coating	300	10.01%	(2018)[43]
Dipropyl sulfide	Overnight	Room Temperature	Doctor blading	~400	9.2 %	(2018)[44]
Dipropyl sulfide	5 hours	Room Temperature	Spin-coating	13	10.8%	(2015)[45]
Dipropyl sulfide	Overnight	Room Temperature	Doctor-blading	~500	16.6 %	(2016)[46]
Dimethyl sulfoxide	2 hours	Room Temperature	Spin-coating	80	4.20%	(2017)[39]
Dipropyl sulfide; Dipropyl sulfide + Chlorobenzene;	Overnight	Room Temperature	Doctor-blading	450	10%	(2017)[47]
Diethyl sulfide	NA	Room temperature	Spin-coating	10-40	11.77%	(2018)[48]
Diethyl sulfide, Ammonia	1 hour	150 ℃	Spin-coating	3-5	10.2%	(2017)[49]
DES solution	NA	Room temperature	Spin-coating	45	7%	(2015)[13]
Diethyl sulfide + Aqueous ammonia	5 hours	Room temperature	Spin coating	30	17.03%	(2019)[50]
Dipropyl sulfide	2 hours	80 ℃	Spin coating	20.5	7%	(2019)[51]

Copper sulphate + sodium thiosulphate	NA	Room temperature	SILAR	NA	0.072%	(2017)[42]
Dipropyl sulfide	NA	150 ℃	Spin coating	45	5%	(2014)[52]

Table 2.6 Table of comparison between different type of HTM in simulation.

Hole transport layer	Solar cell	Thickness, (μm)	Doping (cm^{-3})	Defect density (cm^{-3})	Efficiency (%)	Ref.
Copper(I) Thiocyanate, CuSCN	Solid state-DSSC	0.5	1×10^{18}	NA	16.69	2019 [31]
Copper (I) Iodide, CuI	Solid state-DSSC	0.5	1×10^{18}	NA	17.72	2019 [31]
Copper(I) Thiocyanate, CuSCN	Perovskite	0.1	1×10^{18}	1×10^{15}	25.13	2020 [53]
Copper Oxide, Cu_2O	Perovskite	0.1	1×10^{18}	1×10^{15}	25.41	2020 [53]
Copper(I) Thiocyanate, CuSCN	Perovskite	0.3	1×10^{18}	1×10^{14}	19.32	2020 [54]
Copper(I) Thiocyanate, CuSCN	Perovskite	0.3	1×10^{18}	1×10^{14}	17.03	2019 [50]
Copper(I) Thiocyanate, CuSCN	Perovskite	0.3	1×10^{18}	1×10^{14}	10.01	2018 [43]

2.4 Conclusion

In conclusion, CuSCN as inorganic HTM to be used in solid-state dye- sensitized solar cells is tends to improve the PCE as it can effectively reduce the charge recombination. However, there are many different materials, structures, method, and dyes used in fabrication and simulation process that will produce different performances of SS-DSSC. Thus, various method used in fabrication of CuSCN as hole transport material such as doctor blading method, spin coating method and SILAR method with different efficiency. This shows that CuSCN have high stability and cheaper compared to the Spiro-OMeTAD. Therefore, the outstanding high stability and lifetime of electrons are the reason for developing CuSCN.

Based on the previous work using simulation analysis and fabrication, it shows that the efficiency will affect some parameter such as thickness, doping density, and defect density of hole transport material. This is because Copper (I) Thiocyanate as hole transport layer offers great hole mobility, wider bandgap, cheap cost, and high conductivity technology.

CHAPTER 3:

METHODOLOGY

This methodology chapter provides instructions on the implementation of the information and data obtained using a particular approach for achieving and completing the project goals necessary. In this section, the basic flowchart of this study is also illustrated to encourage and systematically base the project undertaken in orders to achieve more satisfactory and better results. The summary of the approach to be used covering the entire section of this project will be given in this chapter.

3.1 Introduction

This chapter explains and provides the method in implementing and data gathered using simulation to obtain and attain the required project objectives. SCAPS-1D simulation software is employed to design and simulate the devices by using CuSCN as HTL and TiO_2 as ETL in SSDSSC. SCAPS 1D used in this study for studies the efficiency that affects the ETL layer, thickness of HTL layer, different doping density, working temperature and defect interface layer on the main electrical parameters of the SSDSSC. In addition, the various type of absorbent layer and quantum efficiency of different absorbent layer are also investigated. The performance is analyzed through the J-V characteristics that have been obtained.

3.2 Flow chart of the project

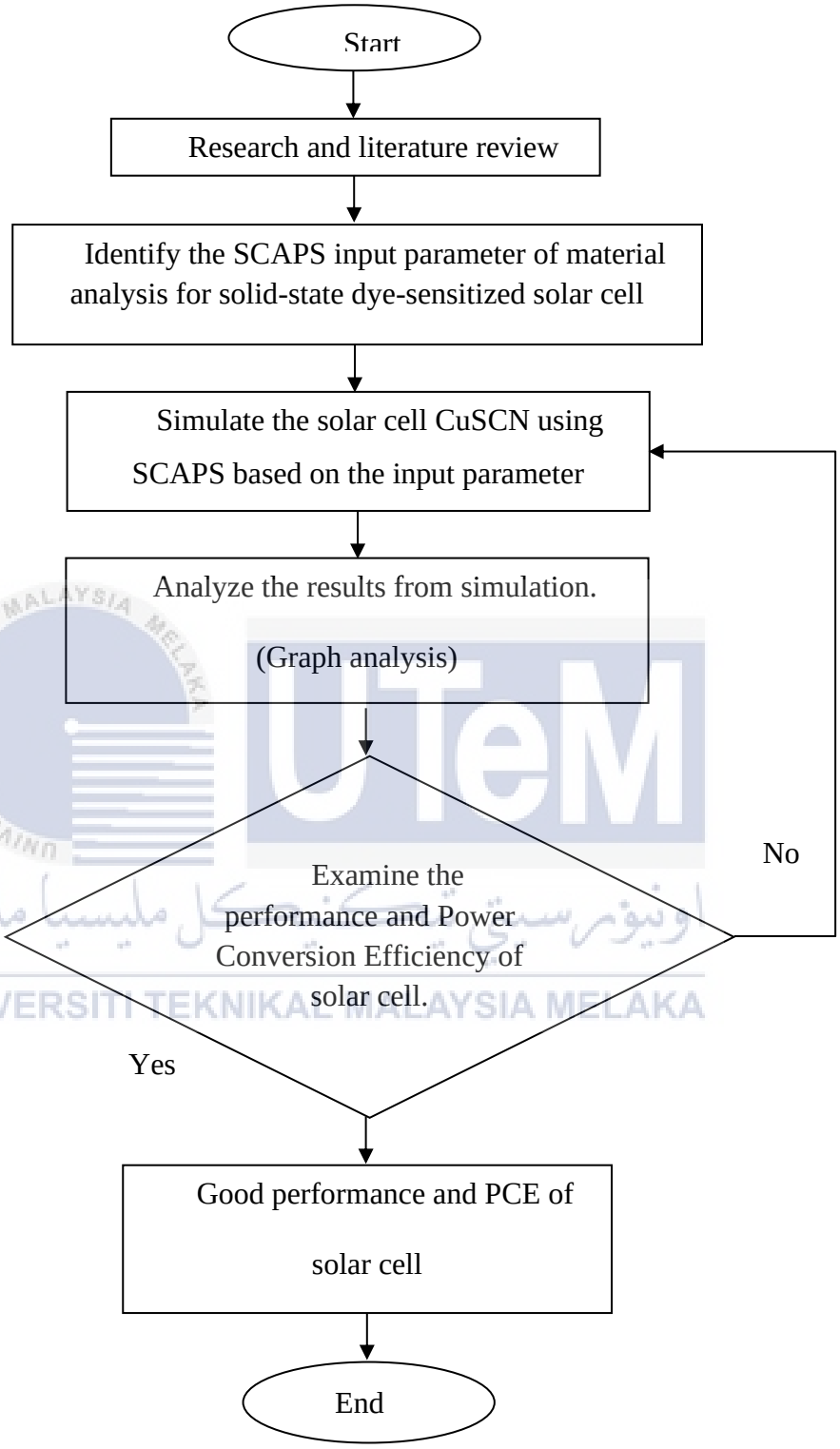

Figure 3.1: Flow chart of project

3.3 SCAPS-1D

Simulation software is valuable and powerful way to investigate the physical structure of a solar cell system without creating a real device. It will save both time and money on system growth. A lot of simulation software has been developed and used to research solar cell systems such as AMPS1D, PC1D, AFORS-HET and so on. SCAPS-1D is a one-dimensional simulation software developed by the University of Gent, Belgium[52]. It has applied to the study of different types of solar cells. Difference between SCAPS with other software which are SCAPS is built in operation window and a lot of models for grading, defects, and recombination.

The main features in SCAPS including materials and defects properties and can insert into 7 layers of material grading, where a lot of grading regulation are given for almost all substance and defect parameters. While the defect definition panel function as to set in both bulky material and interface. There are five different types of defects and the distributions available in the software where it has variety of features that has significant value for solar cells, such as energy bands, concentrations, currents, I-V characteristics, C-V, C-f, and QE can be determined by SCAPS. SCAPS-1D can help most of researchers where it has compliant calculation and collectible data record functionality including single shot, batch calculation, curve fitting, data, and diagram recording.

3.4 Project design

The SCAPS-1D action panel is shown in Figure 3.2 below that consist of for settings:

a) Create a solar cell structure in SCAPS, assess simulated output, record simulated output data, and clear simulated history using the problem definition setting. The set problem button is used to specify the structure of a solar cell.

b) Action settings are used to determine which solar cell measurement to replicate dependent on the user. It consists of J-V calibration setup, C-V capacitance voltage setting, C-F frequency setting and setting of quantum efficiency QE. In this investigation, just the J-V is used determining the efficiency of power conversion (PCE).

c) The illumination setting is utilized for spectrum setting and light direction dark or light. In this investigation, the light in the lighting setting has been activated.

d) Working point setting is used to determine the working temperature.

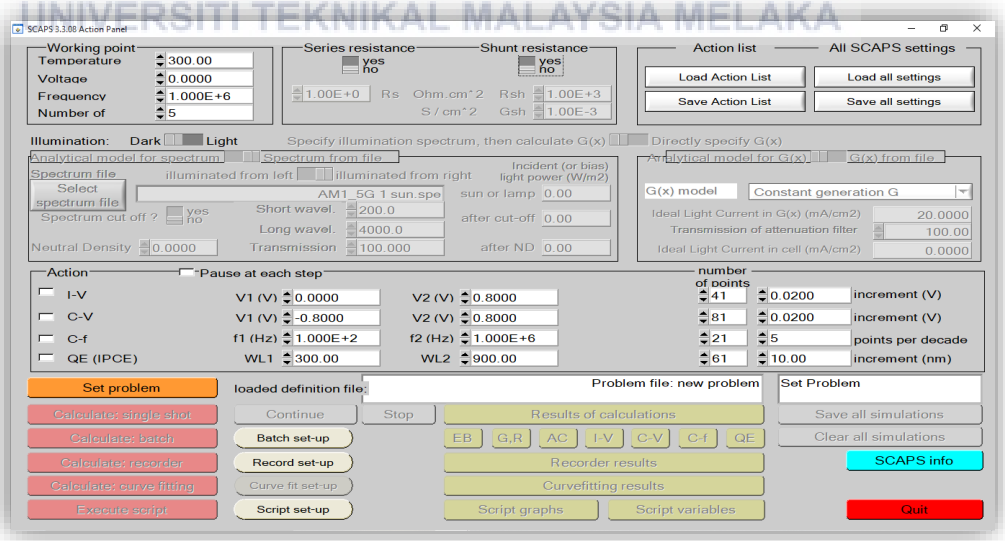

Figure 3.2: SCAPS-1D action panel.

The solar cell definition panel is opened as illustrated in Figure 3.3 after hitting the set problem button. There are three categories in this panel:

a) There are 5 buttons. The function of these buttons is to build new structure files, load and save them in a library for the SCAPS specification. The 'OK' button is clicked when the structure has been defined.

b) It includes layer setting, interface fault, contact attributes (front contact and back contact) and numerical preferences definition. Based on Figure 3.3, it demonstrates that SCAPS-1D supports the structure of solar cells in up to seven layers.

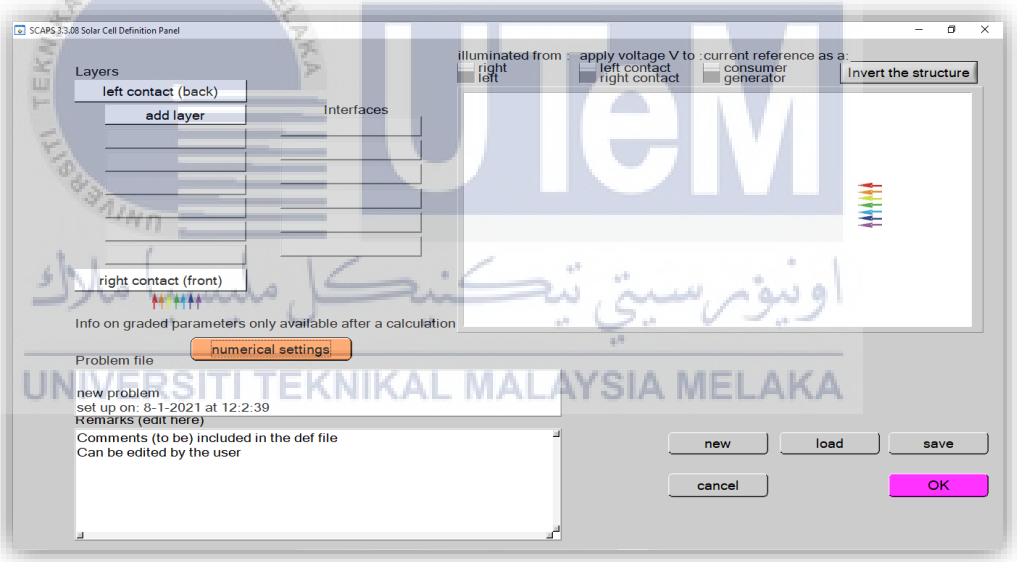

Figure 3.3: Solar cell definition panel.

In this software, the layer properties and parameter are defined in SCAPS-1D layer properties panel as shown in Figure 3.4. In this panel, the parameter of numerical analysis for each layer is set as shown in Table 3.1 based on previous paper

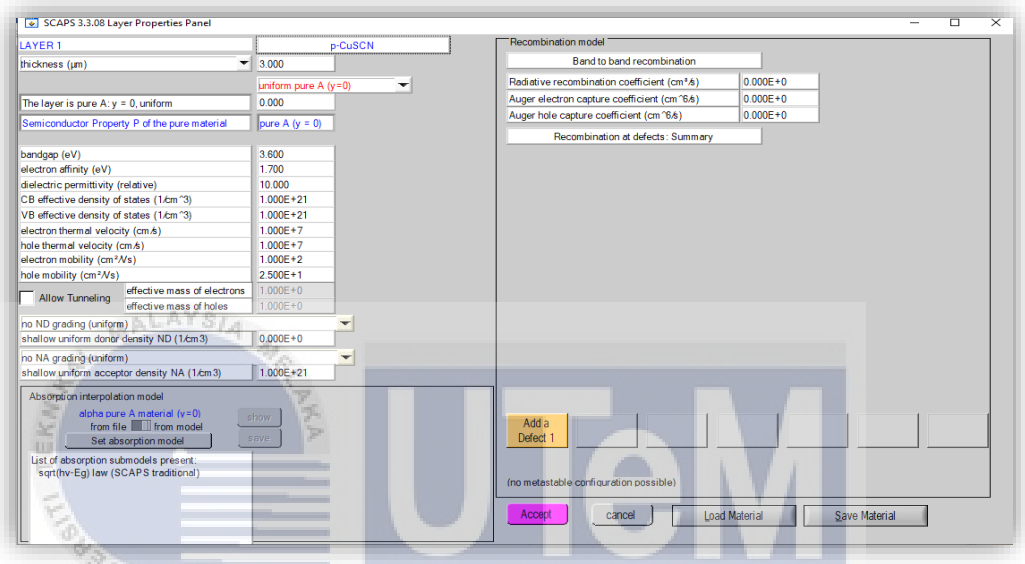

Figure 3.4: Layer properties panel.

3.5 Layers in SCAPS- 1D simulation

In this study, there are 5 layers employed in a composition of device modelling SSDSSCs. The layer consists of FTO as front contact, CuSCN as hole transport layer (p-layer), N719 as a dye-sensitizer, TiO_2 as ETL (n-layer) and Ni a semiconducting material for back contact as shown in Figure 3.5. However, different layer of SSDSSC modelling contain different properties parameter. There are a few parameters that has been analyzed to obtain the optimum efficiency of SSDSSC based on the factor of the presence of Ni as a back contact. The parameters mentioned are such as the various

ETL, thickness of CuSCN, doping density of CuSCN, the working temperature of a solar cell, and a defect interface at each layer.

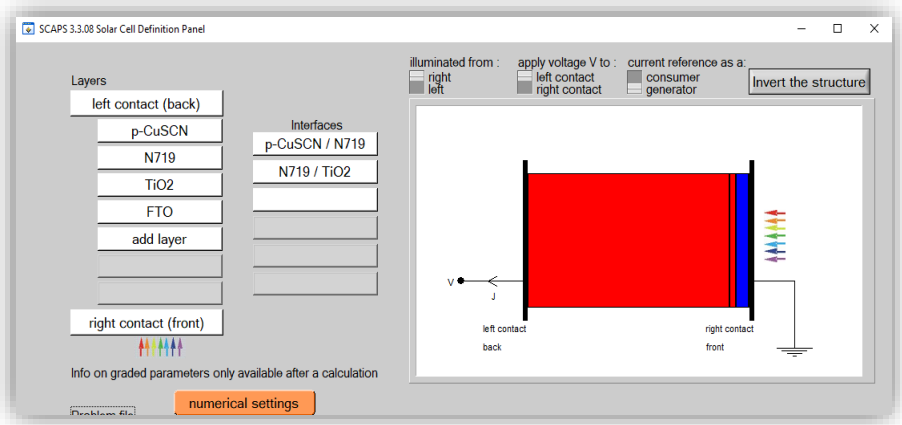

Figure 3.5 Simulated device structure of SSDSSC

3.5.1 Parameters in simulation.

Table below shows the parameter is characteristic that are fixed for the material and the parameter that is required to insert into SCAPS-1D software. All the parameter required from the research which are layer thickness, d (μm), bandgap energy, E_g (eV), electron affinity, (eV), dielectric permittivity, ε (relative), effective density of conduction band, Nc (cm^{-3}), effective density of valence band, Nv (cm^{-3}), thermal velocity of electrons, V_e (cm/s), thermal velocity of holes, V_h (cm/s), electron mobility, μ_e (cm^2/V_s), hole mobility, μ_h (cm^2/V_s), density of donors, N_D (cm^{-3}), and density of acceptors, N_A (cm^{-3}).

Table 3.1: SCAPS-1D input parameter of numerical analysis for SSDSSC

Layer	**TiO_2** [31]	**CuSCN** [31]	**N719** [31]	**ZnO** [55]	**SnO_2** [55]
Layer thickness, d (μm)	0.1	0.5	0.05	0.1	0.1
Bandgap energy, E_g (eV)	3.2	3.6	2.37	3.35	3.6
Electron affinity, (eV)	3.9	1.7	3.9	4.5	4
Dielectric permittivity, ε (relative)	9	10	30	9	9
Effective density of conduction band, Nc (cm^{-3})	1×10^{19}	1×10^{21}	2.5×10^{20}	2.2×10^{18}	2.2×10^{18}
Effective density of valence band, Nv (cm^{-3})	1×10^{19}	1×10^{21}	2.5×10^{20}	1.8×10^{19}	1.8×10^{19}
Thermal velocity of electrons, V_e ($cm\ s^{-1}$)	1×10^{7}	1×10^{7}	1×10^{7}	1×10^{7}	1×10^{7}
Thermal velocity of holes, V_h ($cm\ s^{-1}$)	1×10^{7}	1×10^{7}	1×10^{7}	1×10^{7}	1×10^{7}
Electron mobility, μ_e (cm^2/V_s)	20	100	5	100	100
Hole mobility, μ_h (cm^2/V_s)	10	25	5	25	25
Density of donors, N_D (cm^{-3})	1×10^{16}	NA	NA	1×10^{19}	1×10^{17}
Density of acceptors, N_A (cm^{-3})	NA	1×10^{18}	1×10^{17}	NA	NA

Table 3.2 Parameter for absorbent layer in device modelling of SSDSSC

Parameter	**$CH_3NH_3SnI_3$** [55]	**$CH_3NH_3PbI_3$** [55]
Layer Thickness (μm)	1	1
Bandgap energy,Eg (eV)	1.30	1.50
Electron affinity, (eV)	4.20	3.9
Dielectric permittivity, $\varepsilon\ (relative)$	10	10
Effective density of conduction band, Nc (cm^{-3})	1×10^{18}	2.25×10^{18}
Effective density of valence band, Nv (cm^{-3})	1×10^{18}	1×10^{18}
Thermal velocity of electrons, V_e ($cm\ s^{-1}$)	1×10^{7}	1×10^{7}
Thermal velocity of holes, V_h (cms^{-1})	1×10^{7}	1×10^{7}
Electron mobility, μ_e (cm^2/Vs)	1.6	2.2
Hole mobility, μ_h (cm^2/Vs)	1.6	2.2
Density of donors, N_D (cm^{-3})	NA	NA
Density of acceptors, N_A (cm^{-3})	3.2×10^{15}	1×10^{18}

Lastly, the J-V curve pattern is noticed after program execution and the data will be collected and analyzed. In this investigation, only the power conversion efficiency (PCE) of the shown J-V curve pattern is recorded. If the output doesn't match the expected output, the procedures must be repeated until reach the desired output.

3.6 Method Analysis

The critical parameter values of CuSCN as HTL and TiO_2 as ETL were explored to attain the best efficiency for SSDSSC with the presence and absence of back contact. The parameters involved include the various ETL, thickness of CuSCN, doping density of CuSCN, the operating working temperature of the solar cell, and a defect interface at each layer. Besides, the performance of SSDSSC also was conducted with the influence of different absorbent layer. In addition, the quantum efficiency of different absorbent also was investigated.

3.6.1 Effect different ETL layer

Various forms of ETL can be built into the simulated solar cell device construction. However, several ETLs produce varied results for SSDSSC performance. This study carried out 3 well-known ETLs to be included into the simulated device layer topology. TiO_2, ZnO and SnO_2 are the three ETLs. SSDSSC performance with each ETL has been recorded and analyzed.

3.6.2 Effect various back contact material

The presence of a back contact has a significant impact on SSDSSC's performance. The occurrence of a back contact is noticed and analyzed in this study. Next, the absence of back contact is compared. Nickel with a metal work function of 5.24 eV is used as back contact.

3.6.3 Effect thickness of CuSCN layer

In this study, only the CuSCN thickness layer was altered while other component thicknesses stay fixed. The thickness range was initially analyzed at 0.1 μm to 100 μm, to observe the trend in SSDSSC efficiency with and without back contact and get the optimal CuSCN thickness based on highest efficiency.

3.6.4 Analysis of Doping Density

Usually, the greater doping density can lead to a drop in conductivity due to higher carrier concentrations. Doping density occurred at both HTM and ETL where in HTM it has a density of acceptor, N_A and ETL it has density of donors, N_D. In this study, the value of N_A was varied with a range between 1×10^{14} cm^{-3} to 1×10^{21} cm^{-3}.

3.6.5 Effect working temperature

The efficiency of the solar cell's power conversion is also affected by its working temperature. To get the best power conversion efficiency, the working temperature for both SSDSSC with and without back contact of Ni is varied between 300 K and 360 K. The SSDSSC's temperature Kelvin is the unit of measurement.

3.6.6 Defect interface layer (Neutral)

Considered one type of defect density interface, neutral, was examined in this study. There are two different types of defect interface layers that have been examined. The first defect interface was discovered between CuSCN and N719 dye, while the second was discovered between N719 dye and TiO_2. Total density, which has been integrated over all energies, has been investigated for the first time in the region of 10^2 to 10^{12} cm^{-2}. Meanwhile, the second flaw was found at a distance of 10^{10} to 10^{18} cm^{-2}. If the defect interface value is too high, the simulation will show the convergence failure.

3.6.7 Quantum efficiency

Quantum efficiency can be used to assess the performance of solar cells. In general, quantum efficiency is defined as the ratio of the number of electrons caught by the contacts to the number of incident photons under short-circuit illumination with a single wavelength. [31] Quantum efficiency is measured in nanometers and is characterized as a function of wavelength. The quantum efficiency of three absorbent layers, N719 dye, $CH_3NH_3PbI_3$, and $CH_3NH_3SnI_3$, was investigated in this study.

CHAPTER 4:

RESULTS AND DISCUSSION

This chapter will discuss the result that has been successfully reached. The manufacturing and modelling phase of this project. In addition, this chapter are analyzed and discussed different parameters to obtain a better performance of the device. In addition, there was a similar hypothesis and problem in this project it will be discussed as well.

4.1 Analysis of optimum parameter for SSDSSC of Copper(I) Thiocyanate.

Initially, the crucial process which is to obtain an optimum parameter for SSDSSC component has been carried out. In this study, only the efficiency value (PCE) of the solar cell was recorded and analyzed from the J-V curve obtained. The optimum value of the parameter obtained were used for the following process to find maximum efficiency of SSDSSC with influence of Ni as a back contact.

4.1.1 Analysis of different electron transport layer (ETL)

The analysis of electron transport layer (ETL) is measured by varying the efficiency of different ETL material such as TiO_2, ZnO and SnO_2. Figure 4.1 below stated the J-V curve for the performance of SSDSSC with and without back contact of different ETL involved. Meanwhile, the Table 4.1 shows the performance of SSDSSC with different ETL.

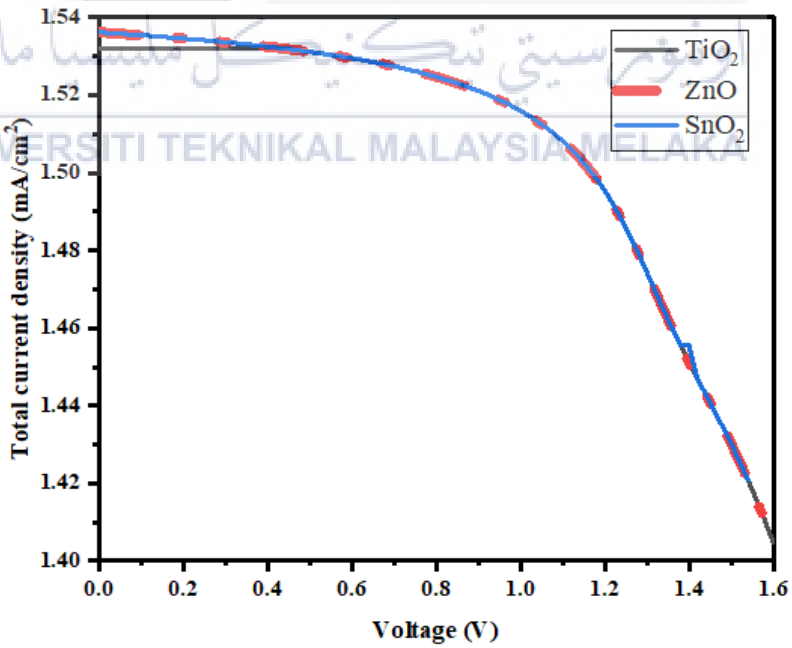

Figure 4.1 J-V curve from different ETL.

The J-V characteristic curve was obtained by SCAPS simulation of the data given in Table 4.1 for different ETL layer. From Figure 4.1 shows that TiO_2 is more optimized results as compared to other ETL layers. However, TiO_2 as ETL are highly efficient but the recombination rate is also quite high because of poor mobility of electron and transport characteristics [56]. The Jsc value for TiO_2 was obtained to be 1.5361 mA/cm^2 which is quite smaller than others ZnO and SnO_2 having 1.5372 $mA/cm^2$and 1.5373 mA/cm^2 respectively. The V_{oc} did not change much. The TiO_2 was shown the optimum PCE of 2.34% among all other ETLs. Hence, TiO_2 can be good alternative for ETL layer.

Table 4.1 The performance of different ETL layers.

ETL	Voc (V)	Jsc (mA/cm^2)	FF (%)	PCE (%)
TiO_2	6.7795	1.536161	22.45	2.34
ZnO	6.7884	1.537161	21.06	2.20
SnO_2	6.7895	1.537261	21.05	2.18

4.1.2 Analysis of different back contact

In this study, various type of back contact has been used to simulate the device structure of the SSDSSC. Each back contact gives different efficiency of solar cells based on their characteristics. Thus, the efficiency obtained from the simulation method is shown in Table 4.3. Besides, the set parameter value of CuSCN for SSDSSC with and without the presence of back contact is shown in Table 4.2 Next, Figure 4.2 below illustrates a graph for performance of SSDSSC efficiency with different of back contact.

Table 4.2 Set parameter value of CuSCN for SSDSSC with back contact

Set parameter	With back contact
Thickness of CuSCN (μm)	0.5
Density of acceptors, N_A (cm^{-3})	1×10^{21}
Working temperature (K)	300

Table 4.3 The efficiency of SSDSSC at different back contact material.

Back contact material	**Ag**	**Fe**	**Cu**	**Au**	**Ni**	**Pt**
Efficiency (%)	2.15	2.15	2.15	2.34	2.55	2.55

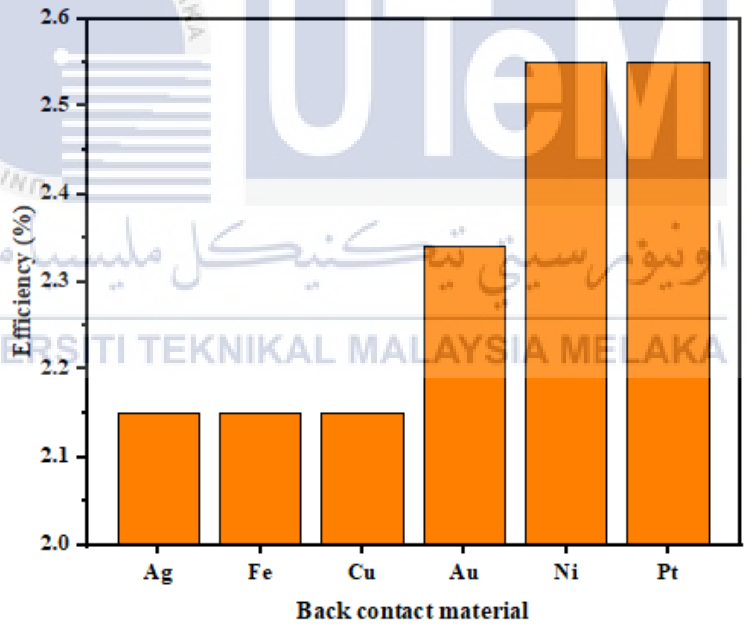

Figure 4.2 The efficiency of SSDSSC obtained from variation back contact material

Based on figure 4.2 above, both Nickel and Platinum gave the same value of efficiency and higher efficiency among the other back contact which is 2.55%. This

shown that as the higher the metal work function of back contact, the highest efficiency of SSDSSC obtained. Thus, the bulk of the carrier barrier height lowers owing to bending bands at the metal semi-conductor interface and therefore increases ohmic contact. [55] Therefore, the materials are relating to a circuit element. In this study, Ni was chosen as the optimum value for back contact materials in this project due to the abundance of using this material that can get lower price than Pt and Ni is also non-toxic materials which is safe to used.

4.1.3 Analysis of variation thickness of CuSCN layer

The analysis of thickness is measured by varying the layer thickness of CuSCN with and without back contact, the thickness went from a range of 0.1 to 100 µm. Table 4.4 shows the set parameter value to plot the thickness graph of hole transport layer.

Table 4.4 Set parameter value for both SSDSSC

Set parameter	With back contact	Without back contact
Thickness of CuSCN (μm)	Variable	Variable
Density of acceptors, N_A (cm^{-3})	1×10^{21}	1×10^{21}
Working temperature (K)	300	300

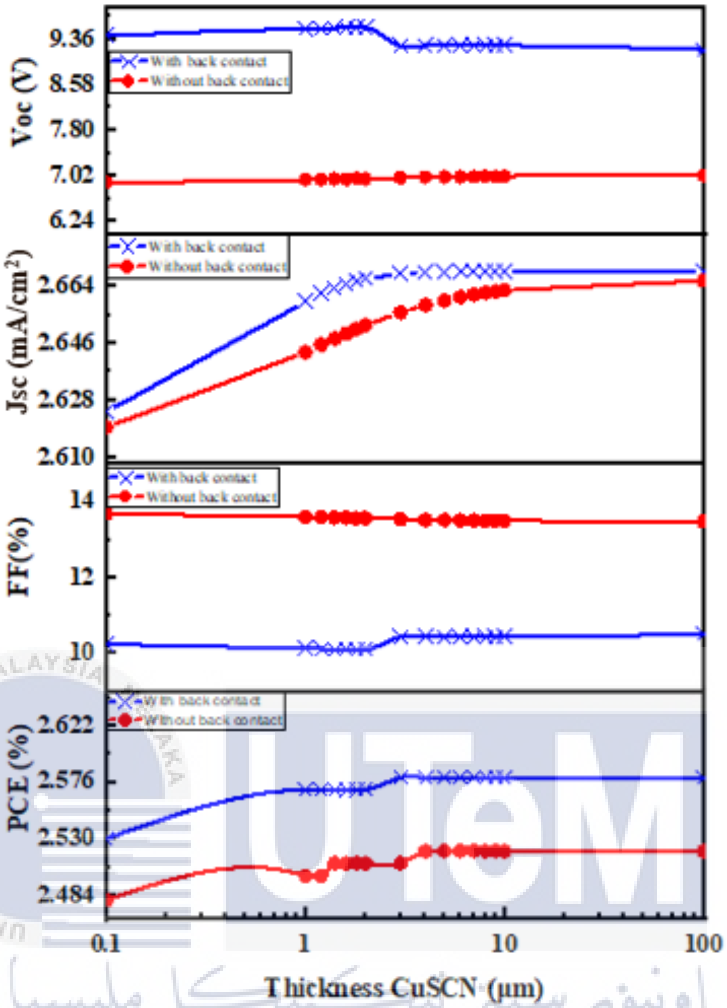

Figure 4.3 The effect of CuSCN layer thickness on (a) open circuit voltage (Voc), (b) short circuit current (Jsc), (c) fill factor (FF) and (d) efficiency (PCE%) of SSDSSC.

Table 4.5 The efficiency of SSDSSC for both with and without back contact at different thickness of CuSCN layer.

Thickness of CuSCN (μm)	Efficiency (%)	
	With back contact	Without back contact
0.1	2.53	2.48
1	2.57	2.5
1.2	2.57	2.5
1.4	2.57	2.51
1.6	2.57	2.51
1.8	2.57	2.51
2	2.57	2.51
3	2.58	2.51
4	2.58	2.52
5	2.58	2.52
10	2.58	2.52
100	2.58	2.52

Figure 4.3 illustrates the effect of CuSCN thickness on various SSDSSC parameters. The thickness varies between 0.1 to 100 μm, and its effect on the Jsc, Voc, FF and PCE of SSDSSC have been investigated. By using this approach, the optimal thickness of CuSCN cells can be obtained. The graphical results obtained show that the V_{oc} increases in the thickness range of 0.1 to 3 μm for back contact and 0.1 to 4 μm for without back contact meanwhile the V_{oc} remain decreases and stable for both with and without back contact from thickness 3 to 100 μm and 4 to 100 μm respectively. This is because when the thickness of CuSCN increases the absorption of photon into the SSDSSC were increase too. Thus, electron will receive enough energy to jump into the conduction band and leave a hole in the valence band. Therefore, more electron-hole pairs will be created in the depletion region [31]. These will gain an excess of carrier concentration and generate higher Jsc that leads to the higher efficiency of SSDSSC.

Based on PCE (%) that obtained in Figure 4.5, both SSDSSC with and without back contact has achieved maximum efficiency which are 2.58% and 2.52% at 3 μm and 4 μm of thickness. Therefore, the optimal thickness chosen for with back contact is 3 μm and without back contact at 4 μm as the efficiency remain constant after the chosen thickness.

4.1.4 Analysis different doping density

A doping density of acceptor denoted by N_A for CuSCN has been varied in a range between 1×10^{14} cm^{-3} to 1×10^{21} cm^{-3} to observe the best efficiency of solar cell. Table 4.6 below shows the set parameter for both SSDSSC with and without the presence of back contact. The result obtained from the simulation in SCAPS-1D software for the analysis of doping acceptor density is shown in Table 4.7. Meanwhile, Figure 4.6 is the effect of efficiency based on different doping density of CuSCN on (a) open circuit voltage (Voc), (b) short circuit current (Jsc), (c) fill factor (FF) and (d) efficiency (PCE%) for with and without back contact of SSDSSC.

Table 4.6 Set parameter value for both SSDSSC

Set parameter	With back contact	Without back contact
Thickness of CuSCN (μm)	3	4
Doping density of acceptors, N_A (cm^{-3})	Variable	Variable
Working temperature (K)	300	300

Table 4.7 The efficiency for both with and without back contact at different doping acceptor density of CuSCN layer

Doping density of CuSCN (cm^{-3})	Efficiency (%)	
	With back contact	Without back contact
1×10^{14}	2.46	2.49
1×10^{15}	2.47	2.49
1×10^{16}	2.49	2.49
1×10^{17}	2.51	2.49
1×10^{18}	2.52	2.5
1×10^{19}	2.54	2.51
1×10^{20}	2.56	2.55
1×10^{21}	2.58	2.57

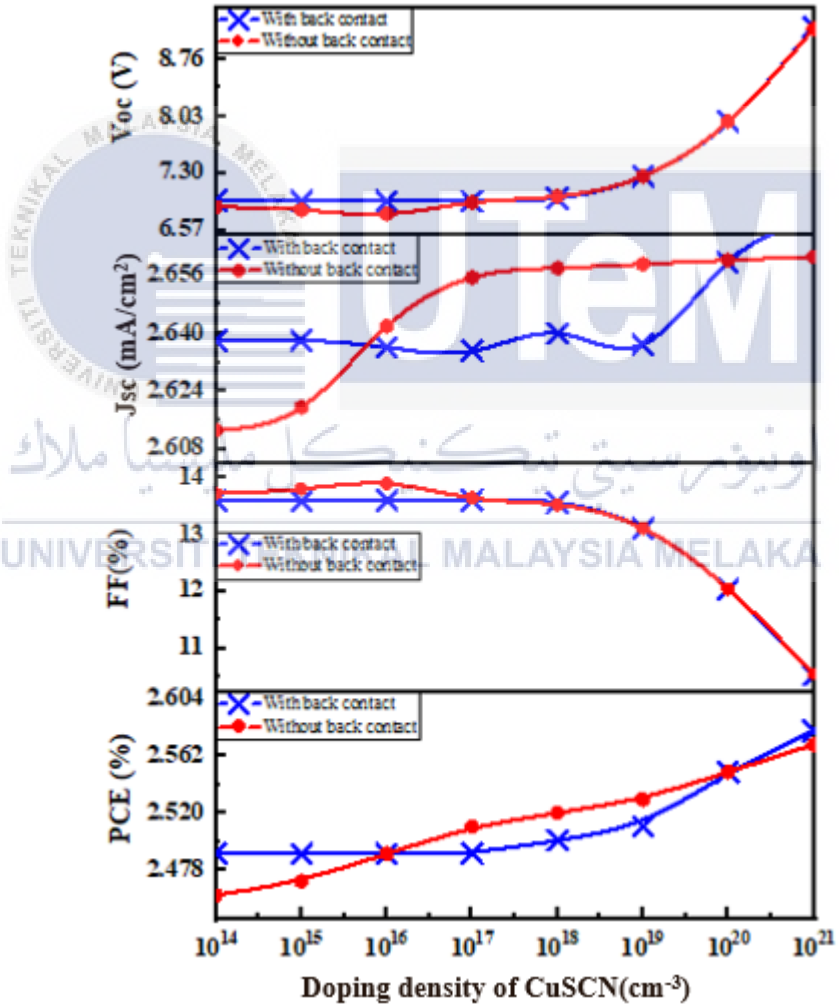

Figure 4.4 The effect of efficiency based on different doping density of CuSCN on (a) open circuit voltage (Voc), (b) short circuit current (Jsc), (c) fill factor (FF%) and (d) efficiency (PCE%) of SSDSSC

Based on Figure 4.6 above, the efficiency of solar cell will increase along with the increasing of doping density of acceptor of CuSCN for both with and without back of SSDSSC structure. This is due to the increase in the conductivity of the cell which leads to a reduction in series of resistance as the density of the doping is increased [31]. The decrease in series resistance is also apparent in a substantial change in the solar cell fill factor (FF) due to an increase in the concentration of doping [31].

By using this approach, the optimal doping acceptor density of CuSCN for both with and without the presence of back contact achieved at 1×10^{21}cm^{-3} which is the efficiency obtained is 2.58% and 2.57% respectively.

4.1.5 Analysis of working temperature

Another factor that influences SSDSSC's photovoltaic performance is working temperature, which is closely related to thermal energy. In this study the working temperature of solar cell has been varied from 300 K to 360 K to analyze the performance of solar cell. Table 4.8 shows the set parameter value for both SSDSSC with and without back contact, while Table 4.9 shows the result obtained for SSDSSC performance with and without back contact as a function of operating temperature fluctuation. Figure 4.5 depicts the graph produced from the variation in working temperature of solar cells.

Table 4.8 The set parameter value for both SSDSSC with and without back contact

Set parameter	With back contact	Without back contact
Thickness of CuSCN (μm)	3	4
Density of acceptors, N_A (cm $^{-3}$)	1×10^{21}	1×10^{21}
Working temperature (K)	Variable	Variable

Table 4.9 The efficiency of SSDSSC for both with and without back contact at different working temperatures

Working Temperature (K)	Efficiency (%)	
	With back contact	Without back contact
300	2.58	2.57
310	2.58	2.57
320	2.57	2.55
330	2.57	2.55
340	2.57	2.5
350	2.53	2.5
360	2.52	2.49

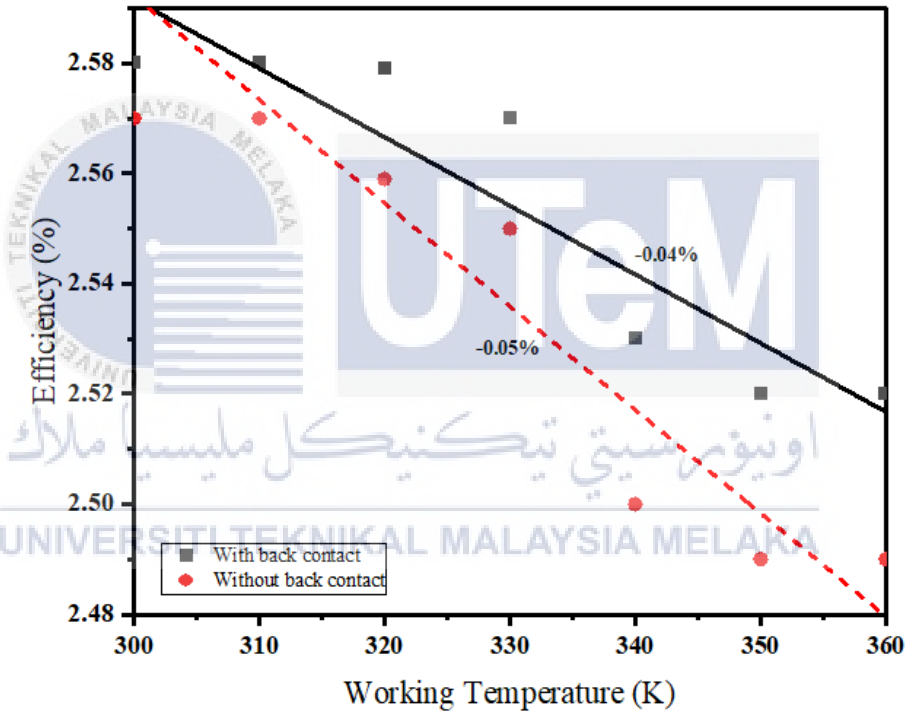

Figure 4.5 The variation of working temperature with and without the presence of Ni as a back contact against the efficiency of SSDSSC

Based on Figure 4.7 shows the same trend as the working temperature increases, the efficiency of solar cell will decrease with trend of approximately -0.05% for without back contact and -0.04% with back contact which is excellent compared to the silicon solar cells -0.4% [57]. As the temperature increase, the bandgap of the semiconductors decreases, causing the crystal lattice to expand and the interatomic

bond to weaken [57][31]. This leads the thermal energy to increase, excites more electron to the conduction band easily and resulting in a high concentration of intrinsic carriers while causing the saturated current to increase [31]. Therefore, the optimal working temperature of the device for both with and without the presence of back contact Ni is 300 K where the efficiency of SSDSSC that has been achieved is 2.58% and 2.57% respectively.

4.1.6 Analysis on defect interface layer

The data obtained from the simulation is observed and recorded in Table 4.11 and Table 4.12, whereas the graph demonstrated in Figure 4.6 below shows the graph analysis of varied defect density for both SSDSSC with and without back contact at CuSCN/N719 interface layer while Figure 4.7 shows the defect on N719 dye/TiO_2 interface layer. The set parameter value for plotting the defect density graph for SSDSSC is shown in Table 4.10.

Table 4.10 The set parameter value for both SSDSSC with and without back contact

Set parameter	With back contact	Without back contact
Thickness of CuSCN (μm)	Variable	Variable
Density of acceptors, N_A (cm^{-3})	1×10^{21}	1×10^{21}
Working temperature (K)	300	300

Table 4.11 Analysis of efficiency based on different defect density at CuSCN/N719 dye for both SSDSSC

Defect interface CuSCN-N719Dyes (cm^{-2})	Efficiency (%)	
	With back contact	Without back contact
1×10^{2}	2.57	2.57
1×10^{4}	2.57	2.57
1×10^{6}	2.57	2.57
1×10^{8}	2.57	2.57
1×10^{10}	2.56	2.56
1×10^{12}	2.11	2.11

Table 4.12 Analysis of efficiency based on different defect density at N719 dye/TiO_2 for both SSDSSC

Defect interface N719-TiO_2 (cm^{-2})	Efficiency (%)	
	With back contact	Without back contact
1×10^{10}	2.57	2.57
1×10^{12}	2.57	2.57
1×10^{14}	2.57	2.57
1×10^{16}	2.56	2.56
1×10^{18}	1.81	1.81

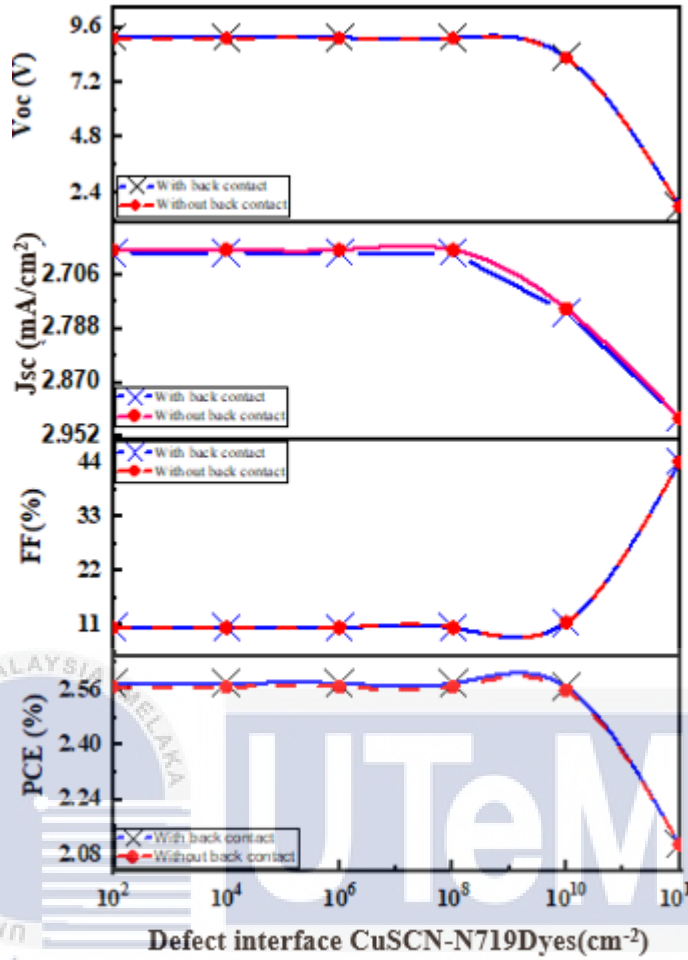

Figure 4.6 The variation of defect density at CuSCN/N719 dye on (a) open circuit voltage (Voc), (b) short circuit current (Jsc), (c) fill factor (FF) and (d) efficiency (PCE%) of SSDSSC against the efficiency of SSDSSC

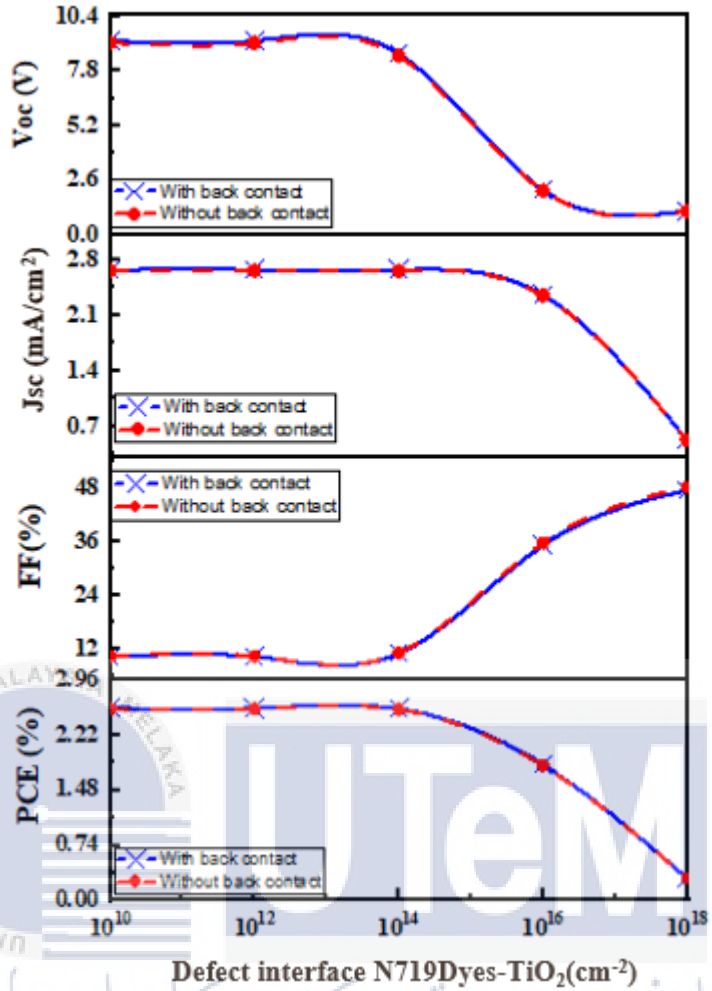

Figure 4.7 The variation of defect density at N719 dye/ TiO_2 (a) open circuit voltage (Voc), (b) short circuit current (Jsc), (c) fill factor (FF) and (d) efficiency (PCE%) of SSDSSC against the efficiency of SSDSSC

Considering the type of defect neutral for both defect interface layer. Based on Figure 4.6 and 4.7, the graph displays that the trend is quite similar, however the drop of defects is difference, this shown that the increase in the defect density of both SSDSSC solar cell resulted in decreases in efficiency for both with and without back contact at difference interface layer. It is because defects affect solar cell efficiency by enabling light to create heat rather than electricity through new recombination pathways (loss) [31][55]. Furthermore, a high carrier diffusion length is caused by a

low defect density concentration [55]. As a result of the low recombination process, solar cell performance has improved.

Thus, the optimum value of defect at interface layer of CuSCN/N719Dye for both with and without the presence of back contact is density at 1×10^8 cm^{-2}. Meanwhile, for the interface layer of N719dye/TiO_2, the optimal value of defect both with and without back contact is 1×10^{14} cm^{-2}.

4.1.7 Analysis of efficiency based on optimum value for all parameters

Table 4.13 below shows the data obtained based on optimum value for all parameters:

Table 4.13 Optimum value for all parameter for both SSDSSC

Parameter	Optimum value	
	With back contact	**Without back contact**
Electron transport layer	TiO_2	TiO_2
Back contact material	Ni (5.24 eV)	NA
Layer thickness CuSCN, d (μm)	3 μm	4 μm
Density of acceptors of CuSCN, N_A (cm^{-3})	1×10^{21}	
Working Temperature (K)	300	
Defect interface 1 (CuSCN-N719Dyes) (cm^{-2}) (Neutral)	1×10^{8}	
Defect interface 2 (N719Dyes/TiO_2) (cm^{-2}) (Neutral)	1×10^{14}	
Open circuit voltage, V_{oc} (V)	1.2790	1.2787
Short-circuit current density, J_{sc} (mA/cm^2)	2.6577	2.6576
Fill factor (%)	75.31	75.32
PCE (%)	2.56	2.56

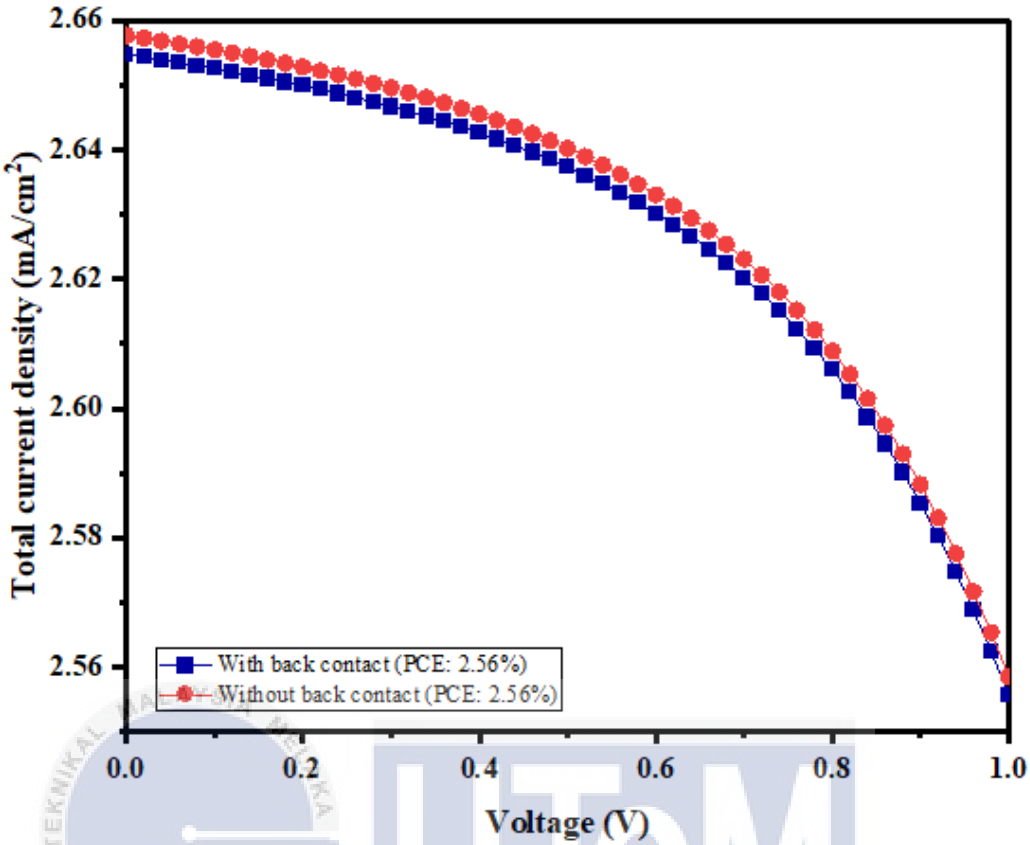

Figure 4.8 J-V curve for optimum value parameters of SSDSSC with and without back contact

The performance of SSDSSC is made from various parameter for HTL layer of CuSCN was studied in this work. The J-V curve for both SSDSSC with and without the presence of back contact Ni is shown in Figures 4.8. By swapping out all the simulation results reveal that CuSCN has the best parameters with the best value.

Based on Figure 4.8 above shows that both SSDSSC with and without back contact has achieved the same optimum efficiency at 2.56%. However, the same optimum efficiency was obtained from different thickness of CuSCN which at which is 3 µm for SSDSSC with back contact and 4 µm for SSDSSC without back contact. Besides, the thickness of CuSCN in SSDSSC with the presence of back contact Nickel is less

than SSDSSC without back contact. Thus, it can be concluded that SSDSSC with back contact is better compared to without back contact solar cell due to the different light reflected at the back contact through the absorber layer which will increase the absorption of light into the cell. However, CuSCN indicates that it is a very adaptable electrical p-type material with great promise for a variety of applications [18]. Hence, the performance of SSDSSC with the presence back contact can be improved as the light capture in the thin TiO_2 has limited the total conversion efficiency of these devices. In this analysis shows that SSDSSC with back contact can conduct with low thickness of CuSCN.

4.2 Analysis of different absorbent layer

In this study, the performance of different absorbent layer for SSDSSC with back contact was investigated further by replacing the N719 dye with perovskite layers such as $CH_3NH_3PbI_3$ and $CH_3NH_3SnI_3$. The performance of SSDSSC with different absorbent layers is shown in Table 4.14, whereas Figure 4.9 displays the performance of SSDSSC with different absorbent layers and shows the J-V curve for the change in absorbent layer for SSDSSC with back contact. Besides, Figure 4.10 illustrates the quantum efficiency for different absorbent layer in SSDSSC that obtained from simulation.

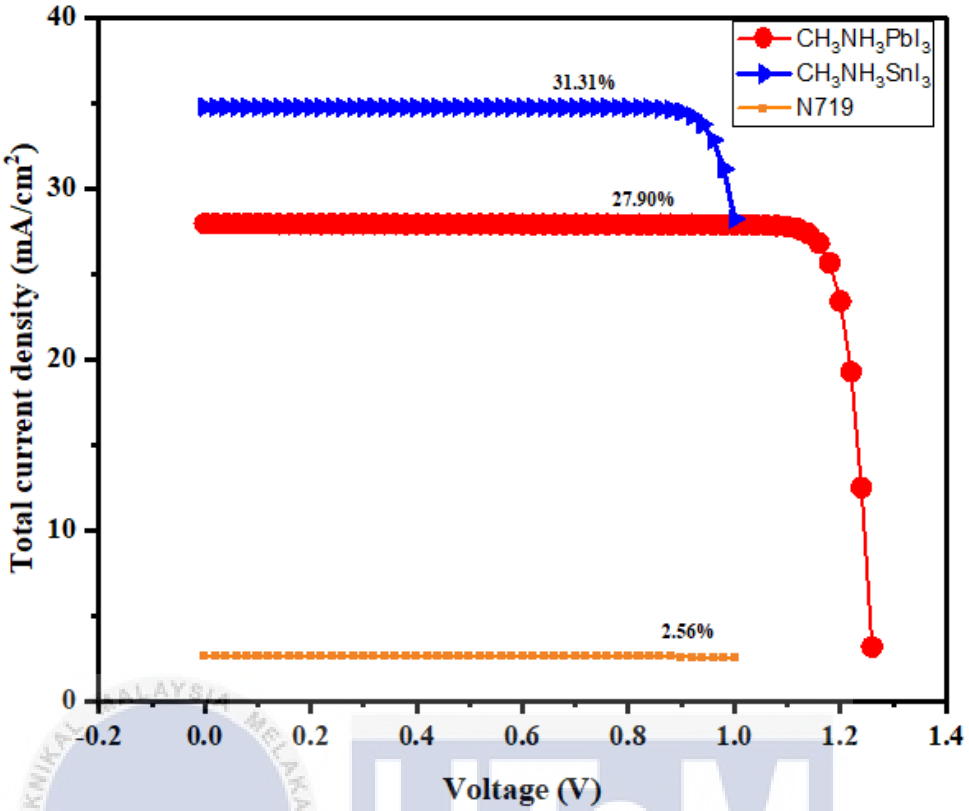

Figure 4.9 J-V curve for different absorbent layer for SSDSSC with the presence of back contact

Table 4.14 Efficiency of different absorbent layer on the performance of SSDSSC with presence back contact

Electron transport layer (ETL)	N719	$CH_3NH_3PbI_3$	$CH_3NH_3SnI_3$
Open circuit voltage, V_{oc} (V)	1.2790	1.2877	1.1967
Short-circuit current density, J_{sc} (mA/cm^2)	2.6577	27.9574	34.1913
Fill factor (%)	75.31	77.50	76.53
PCE (%)	2.56	27.90	31.31

In addition, the performance of different absorber layer such as methyl ammonium lead iodide ($CH_3NH_3PbI_3$) and methyl ammonium tin iodide ($CH_3NH_3SnI_3$) instead of N719 dyes in SSDSSC was analyzed. From the results in Figure 4.9, $CH_3NH_3SnI_3$ has

achieved the highest efficiency which is 31.31%. This shows that $CH_3NH_3SnI_3$ is a potential absorbent layer because it is Pb free, less expansive, and high performance of SSDSSC compared to others absorbent layer. Table 4.14 displays that a perovskite layer $CH_3NH_3SnI_3$ yields the highest efficiency which is 31.31% followed by $CH_3NH_3PbI_3$ which gives the efficiency of 27.90%. However, the N719 layer has the lowest efficiency which is 2.56%.

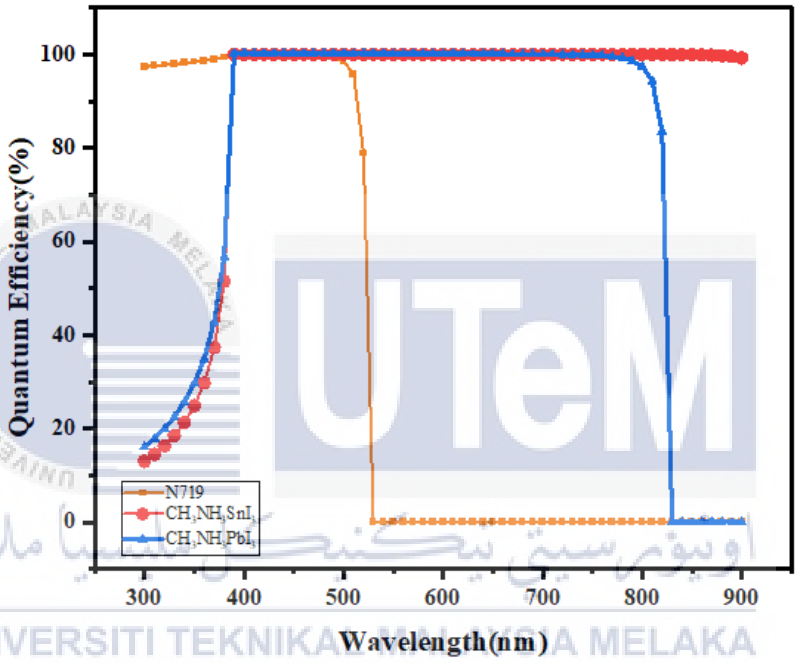

Figure 4.10 Quantum efficiency of different absorbent layer for SSDSSC with presence of back contact

For further studies, the quantum efficiency analysis for different absorber layer also were investigated. The quantum efficiency (QE) can be expressed as a function of wavelength or energy [31]. Based on Figure 4.10, the $CH_3NH_3SnI_3$ shown the best quantum efficiency of the wavelength from 300 nm to 900 nm, this showing that the sunlight has actively absorb by this material. However, $CH_3NH_3PbI_3$ shows that the absorb wavelength only up to 840 nm. Besides, for N719 dyes which have been use in SSDSSC just absorbs wavelength up to 500 nm only compared to others.

4.3 Environment and Sustainability

The economy is the first faces of this project's long-term viability. This is since this project does not require any funds because it is totally simulated utilizing SCAPS software. Next, in terms of the environment, this idea is viable. It is environmentally beneficial because it does not necessitate the use of oil or any other polluting chemical chemicals environment and able to lower emissions of greenhouse gasses without affecting the growth of a country.

CHAPTER 5:

CONCLUSION AND FUTURE WORKS

5.1 Conclusion

Solid-state dye sensitized solar cell (SSDSSC) is categories as third generation of solar cell attribute as the liquid electrolyte is replaced by solid-state hole conducting organic molecule which offers higher stability and reliability. CuSCN as HTL are promising due to its wide bandgap conduction band where it allows the possibility to generate lower resistivity because of its larger surface area.

The main objective of this project is to simulate the CuSCN as inorganic p-type material using SCAPS simulation software based on the SCAPS input parameter numerical analysis. The important parameter values of CuSCN as HTL were examined to obtain the highest efficiency for SSDSSC with the presence of back contact. The parameters involved include the different ETL layer, thickness of CuSCN, doping density of CuSCN, the working temperature of the solar cell, and a defect interface at

each layer. Moreover, further analysis also been made for comparison of different absorbent layer and quantum efficiency for different absorbent layer.

As a result, it shows that of CuSCN without and with back contact produced the same efficiency of 2.56%. However, CuSCN with back contact has better performance than without back contact. Thus, it can be concluded that with the presence of back contact, CuSCN yields better performance of SSDSSC.

5.2 Future Works

In future, the simulation results can be used as a guide in the fabrication method for SSDSSC employing CuSCN as hole transport layer with the presence of back contact Ni. The SSDSSC can also be improved by using a low thickness of HTL and CuSCN as HTL material. Moreover, the simulation results can also be used as a guide to simulate and fabricate the Perovskite Solar Cell by employing CuSCN as HTL.

REFERENCES

[1] G. W. Crabtree and N. S. Lewis, “Solar energy conversion,” *Phys. Today*, vol. 60, no. 3, pp. 37–42, 2007.

[2] M. A. Green, E. M. Keller, J. S. Shi, A. W. Blakers, and S. R. Wenham, “High-Efficiency Silicon Solar Cells,” *IEEE Trans. Electron Devices*, vol. 31, no. 5, pp. 679–683, 1984.

[3] T. Soga, “Fundamentals of Solar Cell,” *Nanostructured Mater. Sol. Energy Convers.*, pp. 3–43, 2006.

[4] K. Ranabhat, L. Patrikeev, A. A. evna Revina, K. Andrianov, V. Lapshinsky, and E. Sofronova, “An introduction to solar cell technology,” *J. Appl. Eng. Sci.*, vol. 14, no. 4, pp. 481–491, 2016.

[5] M. T. Kibria, A. Ahammed, and S. M. Sony, “A Review : Comparative studies on different generation solar cells technology,” *Env. Aspects.*, pp. 51–53, 2014.

[6] M. E. Ragoussi and T. Torres, “New generation solar cells: Concepts, trends and perspectives,” *Chem. Commun.*, vol. 51, no. 19, pp. 3957–3972, 2015.

[7] O. Vigil-Galán, M. Courel, and J. A. Andrade-Arvizu, “Route towards low cost-high efficiency second generation solar cells: current status and perspectives,” *J. Mater. Sci. Mater. Electron.*, vol. 26, no. 8, pp. 5562–5573, 2015.

[8] M. A. Green, “Third generation photovoltaics: Solar cells for 2020 and beyond,” *Phys. E Low-Dimensional Syst. Nanostructures*, vol. 14, no. 1–2, pp. 65–70, 2002.

[9] J. Yan and B. R. Saunders, "Third-generation solar cells: A review and comparison of polymer:fullerene, hybrid polymer and perovskite solar cells," *RSC Adv.*, vol. 4, no. 82, pp. 43286–43314, 2014.

[10] J. E. Jaffe, T. C. Kaspar, and T. C. Droubay, "Electronic and defect structures of CuSCN," *J. Phys. Chem. C*, vol. 114, no. 19, pp. 9111–9117, 2010.

[11] P. Pattanasattayavong and G. O. N. Ndjawa, "Electric field-induced hole transport in copper(I) thiocyanate (CuSCN) thin-films processed from solution at room temperature," *Chem. Commun.*, vol. 49, no. 39, pp. 4154–4156, 2013.

[12] S. P. A. U. K. Samarakoon, P. G. D. C. K. Karunarathna, and C. A. N. Fernando, "Characterization of Fe doped n-CuSCN/p-Cu2S solid-state photovoltaic cell," *Mater. Res. Express*, vol. 5, no. 6, pp. 2–9, 2018.

[13] N. Wijeyasinghe and T. D. Anthopoulos, "Copper(I) thiocyanate (CuSCN) as a hole-transport material for large-area opto/electronics," *Semicond. Sci. Technol.*, vol. 30, no. 10, 2015.

[14] C. S. K. Ranasinghe, E. N. Jayaweera, and G. R. A. Kumara, "Development of dye-sensitized solid-state ZnO/D149/CuSCN solar cell," *Int. J. Nanosci.*, vol. 13, no. 4, pp. 1–6, 2014.

[15] B. O'Regan, F. Lenzmann, and R. Muis, "A solid-state dye-sensitized solar cell fabricated with pressure-treated P25-TiO_2 and CuSCN: Analysis of pore filling and IV characteristics," *Chem. Mater.*, vol. 14, no. 12, pp. 5023–5029, 2002.

[16] M. Kim, S. Park, and J. Jeong, "Band-Tail Transport of CuSCN: Origin of Hole Extraction Enhancement in Organic Photovoltaics," *J. Phys. Chem. Lett.*, vol. 7, no. 14, pp. 2856–2861, 2016.

[17] F. Matebese, R. Taziwa, and D. Mutukwa, "Progress on the Synthesis and Application of CuSCN Inorganic Hole Transport Material in Perovskite Solar Cells," *Materials*, pp. 1-19, 2018.

[18] N. Wijeyasinghe and T. D. Anthopoulos, "Copper (I) thiocyanate (CuSCN)

as a hole-transport material for large-area opto / electronics," *Materials.*, vol. 104002, pp. 1–45, 2015.

[19] J. Zhang, M. Freitag, A. Hagfeldt, and G. Boschloo, "*S*olid-State Dye-Sensitized Solar Cells*" Sol. Energy*, pp. 151-185, 2018.

[20] R. Jose, V. Thavasi, and S. Ramakrishna, "Metal oxides for dye-sensitized solar cells," *J. Am. Ceram. Soc.*, vol. 92, no. 2, pp. 289–301, 2009.

[21] D. Moia, U. B. Cappel, and T. Leijtens, "The Role of Hole Transport between Dyes in Solid-State Dye-Sensitized Solar Cells," *J. Phys. Chem. C*, vol. 119, no. 33, pp. 18975–18985, 2015.

[22] J. E. Kroeze, N. Hirata, and S. Koops, "Alkyl chain barriers for kinetic optimization in dye-sensitized solar cells," *J. Am. Chem. Soc.*, vol. 128, no. 50, pp. 16376–16383, 2006.

[23] A. S. Hey and H. J. Snaith, "Large area hole transporter deposition in efficient solid-state dye-sensitized solar cell mini-modules," *J. Appl. Phys.*, vol. 114, no. 18, 2013.

[24] B. Li, L. Wang, B. Kang, P. Wang, and Y. Qiu, "Review of recent progress in solid-state dye-sensitized solar cells," *Sol. Energy Mater. Sol. Cells*, vol. 90, no. 5, pp. 549–573, 2006.

[25] A. Listorti, B. O'Regan, and J. R. Durrant, "Electron transfer dynamics in dye-sensitized solar cells," *Chem. Mater.*, vol. 23, no. 15, pp. 3381–3399, 2011.

[26] U. Bach, Y. Tachibana, J. Moser, S. A. Haque, J. R. Durrant, and M. Gra, "Charge Separation in Solid-State Dye-Sensitized Heterojunction Solar Cells," *J. Chem. Soc.*, vol. 2, pp. 7445–7446, 1999.

[27] F. Paquin, J. Rivnay, A. Salleo, N. Stingelin, and C. Silva, "Multi-phase semicrystalline microstructures drive exciton dissociation in neat plastic semiconductors," *J. Mater. Chem. C*, vol. 3, pp. 10715–10722, 2015.

[28] F. Behrouznejad and E. Shahbazi, S. Taghavinia, N. Wu, H. Ping, W. G. Diau,

"A study on utilizing different metals as the back contact of $CH_3NH_3PbI_3$ perovskite solar cells," *J. Mater. Chem. A*, vol. 4, no. 35, pp. 13488–13498, 2016.

[29] B. O'Regan and D. T. Schwartz, "Efficient dye-sensitized charge separation in a wide-band-gap p-n heterojunction," *J. Appl. Phys.*, vol. 80, no. 8, pp. 4749–4754, 1996.

[30] G. R. R. A. Kumara, A. Konno, G. K. R. Senadeera, P. V. V. Jayaweera, D. B. R. A. De Silva, and K. Tennakone, "Dye-sensitized solar cell with the hole collector p-CuSCN deposited from a solution in n-propyl sulphide," *Sol. Energy Mater. Sol. Cells*, vol. 69, no. 2, pp. 195–199, 2001.

[31] F. Jahantigh and M. J. Safikhani, "The effect of HTM on the performance of solid-state dye-sanitized solar cells (SDSSCs): a SCAPS-1D simulation study," *Appl. Phys. A Mater. Sci. Process.*, vol. 125, no. 4, pp. 1–7, 2019.

[32] X. Isakov, I. Paterson, A. F. Solomeshch, O. Tessler, N. Zhang, Q. Li, J. Zhang, M. Fei, Z. Heeney, and T. D. Anthopoulos, "Hybrid complementary circuits based on p-channel organic and n-channel metal oxide transistors with balanced carrier mobilities of up to 10 cm^2/Vs," *Appl. Phys. Lett.*, vol. 109, no. 26, pp. 1–5, 2016.

[33] S. Ruzgar, Y. Caglar, and M. Caglar, "The influence of low indium composition ratio on sol–gel solution-deposited amorphous zinc oxide thin film transistors," *J. Mater. Sci. Mater. Electron.*, vol. 31, no. 14, pp. 11720–11728, 2020.

[34] T. Lin, X. Li, and J. Jang, "High performance p-type NiOx thin-film transistor by Sn doping," *Appl. Phys. Lett.*, vol. 108, no. 23, pp. 1–5, 2016.

[35] S. Jenifer, K. Arulkumar and J. Y. Parthiban, S.Kwon, "A Review on the Recent Advancements in Tin Oxide-Based Thin-Film Transistors for Large-Area Electronics," *J. Electron. Mater.*, vol. 49, no. 12, pp. 7098–7111, 2020.

[36] J. H. Kim, "High-performance and environmentally stable planar heterojunction perovskite solar cells based on a solution-processed copper-

doped nickel oxide hole-transporting layer," *Adv. Mater.*, vol. 27, no. 4, pp. 695–701, 2015.

[37] B. J. Park, S. Kim and N. K. Kang, S. J. Cho, "Photocurrent Characteristics of Zinc-Oxide Films Prepared by Using Sputtering and Spin-Coating Methods," *J. Korean Phys. Soc.*, vol. 73, no. 9, pp. 1351–1355, 2018.

[38] A. Augusto and C. Herasimenka, S. Y. King, R. R. Bowden, S. G. Honsberg, "Analysis of the recombination mechanisms of a silicon solar cell with low bandgap-voltage offset," *J. Appl. Phys.*, vol. 121, no. 20, pp. 1–6, 2017.

[39] N. Chaudhary and A. Chaudhary, R. Kesari, J. Patra, "An eco-friendly and inexpensive solvent for solution processable CuSCN as a hole transporting layer in organic solar cells," *Opt. Mater. (Amst).*, 2017.

[40] B. N. Ezaligo, A. C. Nwanya, and S. Aline, "A study on solution deposited CuSCN thin films_ Structural, electrochemical, optical properties." *Journal of Solid State Electrochemistry*, 2017.

[41] P. K. Baviskar, P. R. Nikam, S. S. Gargote, A. Ennaoui, and B. R. Sankapal, "Controlled synthesis of ZnO nanostructures with assorted morphologies via simple solution chemistry," *J. Alloys Compd.*, vol. 551, pp. 233–242, 2013.

[42] P. K. Baviskar, "Low-cost solid-state dye-sensitized solar cell based on ZnO with CuSCN as a hole transport material using simple solution chemistry," *J. Solid State Electrochem.*, 2017.

[43] Y. Lv and H. Guo, Y. Zhang, H. Zhou, X. Chen, "Enhanced efficiency and stability of fully air-processed TiO_2 nanorods array based perovskite solar cell using commercial available CuSCN and carbon," *Sol. Energy*, vol. 173, no. May, pp. 7–16, 2018.

[44] R. Karuppuchamy, S. Murugadoss, G. Ramachandran, K. Saxena, V. Thangamuthu, "Inorganic based hole transport materials for perovskite solar cells," *J. Mater. Sci. Mater. Electron.*, vol. 29, no. 10, pp. 8847–8853, 2018.

[45] Y. Zhao, K.Munir, R.Yan, B.Yang and A. Kim, T.Amassian, "Solution-processed inorganic copper(i) thiocyanate (CuSCN) hole transporting layers for efficient p-i-n perovskite solar cells," *J. Mater. Chem. A*, vol. 3, no. 41, pp. 20554–20559, 2015.

[46] V. E. Madhavan, I. Zimmermann, C. Roldán-Carmona, M. Grancini, G. Buffiere, and M. K. Belaidi, A. Nazeeruddin, "Copper Thiocyanate Inorganic Hole-Transporting Material for High-Efficiency Perovskite Solar Cells," *ACS Energy Lett.*, vol. 1, no. 6, pp. 1112–1117, 2016.

[47] R. Thangamuthu and G. Murugadoss, "Fabrication of $CH_3NH_3PbI_3$ perovskite-based solar cells: Developing various new solvents for CuSCN hole transport material," *Sol. Energy Mater. Sol. Cells*, 2017.

[48] T. Akhtaruzzaman, M. Kayesh, M. E. Lee, J. Joon, "Low temperature processed inverted planar by CuSCN hole transport bilayer with improved stability," *Sol. Energy*, pp. 1-12, 2018.

[49] N. Wijeyasinghe, A. Regoutz, F. Eisner, T. Du, L. Tsetseries, Y. H. Lin, H. Faber, P. Pattanasattayavong, J. Li, F. Yan, M. A. McLachlan, D. J. Payne, M. Heeney and T. D. Anthopoulos., "Copper(I) Thiocyanate (CuSCN) Hole-Transport Layers Processed from Aqueous Precursor Solutions and Their Application in Thin-Film Transistors and Highly Efficient Organic and Organometal Halide Perovskite Solar Cells," *Adv. Funct. Mater.*, vol. 27, no. 35, pp. 1–49, 2017.

[50] A. Montgomery, L. Guo, C. Grice, R. A. Awni, S. Saurav, L. Li, Y. Yan, F. Yan, "Solution-processed copper (I) thiocyanate (CuSCN) for highly efficient CdSe/CdTe thin-film solar cells," *Prog. Photovoltaics Res. Appl.*, vol. 27, no. 8, pp. 665–672, 2019.

[51] K. Li, S.Wang, C. Chen, R. Kondrotas, M. Hu, S. Lu, C. Wang, W. Chen and J. Tang, "7.5% n-i-p Sb2Se3 solar cells with CuSCN as a hole-transport layer," *J. Mater. Chem. A*, vol. 7, no. 16, pp. 9665–9672, 2019.

[52] N. Yaacobi-Gross, N. D. Treat, P. Pattanasattayavong, H. Faber, Ajay K.

Permal, N. Stingelin, D. D. C. Bradley, P. N. Stavrinou, M. Heeney, and T. D. Anthopoulos, “High-efficiency organic photovoltaic cells based on the solution-processable hole transporting interlayer copper thiocyanate (CuSCN) as a replacement for PEDOT:PSS,” *Adv. Energy Mater.*, vol. 5, no. 3, pp. 1–7, 2015.

[53] P. Roy, S. Tiwari, and A. Khare, “An investigation on the influence of temperature variation on the performance of tin (Sn) based perovskite solar cells using various transport layers and absorber layers,” *Results Opt.*, vol. 4, no. March, p. 100083, 2021.

[54] I. Alam and M. A. Ashraf, “Effect of different device parameters on tin-based perovskite solar cell coupled with In2S3 electron transport layer and CuSCN and Spiro-OMeTAD alternative hole transport layers for high-efficiency performance,” *Energy Sources, Part A Recover. Util. Environ. Eff.*, pp. 1–25, 2020.

[55] F. Anwar, R. Mahbub, S. S. Satter, and S. M. Ullah, “Effect of Different HTM Layers and Electrical Parameters on ZnO Nanorod-Based Lead-Free Perovskite Solar Cell for High-Efficiency Performance,” *Int. J. Photoenergy*, vol. 2017, 2017.

[56] G. Yang, H. Tao, P. Qin, W. Ke, and G. Fang, “Recent progress in electron transport layers for efficient perovskite solar cells,” *J. Mater. Chem. A*, vol. 4, no. 11, pp. 3970–3990, 2016.

[57] E. Radziemska, "The effect of temperature on the power drop in cystalline silicon solar cells," *Renewable Energy*, vol. 2002, pp. 1-12, 2002.